

Thieno[3,2-b]pyrrole-5-carboxamides as New Reversible Inhibitors of Histone Lysine Demethylase KDM1A/LSD1. Part 1: High Throughput Screening and Preliminary Exploration

Luca Sartori, Ciro Mercurio, Federica Amigoni, Anna Cappa, Giovanni Fagá, Raimondo Fattori, Elena Legnaghi, Giuseppe Ciossani, Andrea Mattevi, Giuseppe Meroni, Loris Moretti, Valentina Cecatiello, Sebastiano Pasqualato, Alessia Romussi, Florian Thaler, Paolo Trifiró, Manuela Villa, Stefania Vultaggio, Oronza A. Botrugno, Paola Dessanti, Saverio Minucci, Elisa Zagarrí, Daniele Carettoni, Lucia Iuzzolino, Mario Varasi, and Paola Vianello

J. Med. Chem., **Just Accepted Manuscript** • DOI: 10.1021/acs.jmedchem.6b01018 • Publication Date (Web): 10 Feb 2017

Downloaded from <http://pubs.acs.org> on February 11, 2017

Just Accepted

“Just Accepted” manuscripts have been peer-reviewed and accepted for publication. They are posted online prior to technical editing, formatting for publication and author proofing. The American Chemical Society provides “Just Accepted” as a free service to the research community to expedite the dissemination of scientific material as soon as possible after acceptance. “Just Accepted” manuscripts appear in full in PDF format accompanied by an HTML abstract. “Just Accepted” manuscripts have been fully peer reviewed, but should not be considered the official version of record. They are accessible to all readers and citable by the Digital Object Identifier (DOI®). “Just Accepted” is an optional service offered to authors. Therefore, the “Just Accepted” Web site may not include all articles that will be published in the journal. After a manuscript is technically edited and formatted, it will be removed from the “Just Accepted” Web site and published as an ASAP article. Note that technical editing may introduce minor changes to the manuscript text and/or graphics which could affect content, and all legal disclaimers and ethical guidelines that apply to the journal pertain. ACS cannot be held responsible for errors or consequences arising from the use of information contained in these “Just Accepted” manuscripts.

1
2
3
4
5
6
7
8
9
10
11
12
13
14
15
16
17
18
19
20
21
22
23
24
25
26
27
28
29
30
31
32
33
34
35
36
37
38
39
40
41
42
43
44
45
46
47
48
49
50
51
52
53
54
55
56
57
58
59
60

	Experimental Oncology Zagarri, Elisa; Fondazione FADOI Carettoni, Daniele; Axxam, Screening Technologies Iuzzolino, Lucia; Axxam, Screening Technologies Varasi, Mario; IFOM - the FIRC Institute of Molecular Oncology Foundation, Experimental Therapeutics Unit Vianello, Paola; IFOM - the FIRC Institute of Molecular Oncology Foundation, Experimental Therapeutics Unit

SCHOLARONE™
Manuscripts

1
2
3
4
5
6
7
8
9
10
11
12
13
14
15
16
17
18
19
20
21
22
23
24
25
26
27
28
29
30
31
32
33
34
35
36
37
38
39
40
41
42
43
44
45
46
47
48
49
50
51
52
53
54
55
56
57
58
59
60

Thieno[3,2-b]pyrrole-5-carboxamides as New Reversible Inhibitors of Histone Lysine Demethylase KDM1A/LSD1. Part 1: High Throughput Screening and Preliminary Exploration

Luca Sartori,^{,†,§} Ciro Mercurio,^{†,‡,±} Federica Amigoni,[†] Anna Cappa,^{†,‡} Giovanni Fagá,^{†,§} Raimondo Fattori,^{†,§} Elena Legnaghi,[†] Giuseppe Ciossani,[‡] Andrea Mattevi,[‡] Giuseppe Meroni,^{†,§} Loris Moretti,^{†,¶} Valentina Cecatiello,^{⊖,||} Sebastiano Pasqualato,^{||} Alessia Romussi,^{†,‡} Florian Thaler,^{†,§} Paolo Trifiró,^{†,§} Manuela Villa,^{†,§} Stefania Vultaggio,^{†,‡} Oronza A. Botrugno,[†] Paola Dessanti,[†] Saverio Minucci,^{†,⊥} Elisa Zagarri,[†] Daniele Caretoni,[^] Lucia Iuzzolino,[^] Mario Varasi,^{†,§} Paola Vianello^{*,†,‡}*

[†] Department of Experimental Oncology, Academic Drug Discovery, European Institute of Oncology, Via Adamello 16, 20139 Milan, Italy

[‡] Department of Biology and Biotechnology, University of Pavia, Via Ferrata 1, 27100 Pavia, Italy

^{||} Crystallography Unit, Department of Experimental Oncology, European Institute of Oncology, Via Adamello 16, 20139 Milan, Italy

[⊖] IFOM, Fondazione Istituto FIRC di Oncologia Molecolare, Via Adamello 16, 20139 Milano, Italy

[⊥] Department of Biosciences, University of Milan, Via Celoria, 26, 20133 Milan, Italy

[^]Axxam, via A. Meucci 3, 20091 Bresso (MI), Italy

1
2
3 ± Genextra Group, DAC s.r.l., Via Adamello 16, 20139 Milan, Italy

4
5 KEYWORDS: epigenetics; lysine-specific demethylase-1; KDM1A; LSD1; TR-FRET; HTS;
6
7 Reversible inhibitors.
8

9 10 **ABSTRACT**

11
12 Lysine specific demethylase 1 KDM1A (LSD1) is one regulator of histone methylation and it
13
14 is increasingly recognized as a potential therapeutic target in oncology. We report on a high-
15
16 throughput screening campaign performed on KDM1A/CoREST, using a time resolved
17
18 fluorescence resonance energy transfer (TR-FRET) technology, to identify reversible
19
20 inhibitors. The screening led to 115 hits for which we determined biochemical IC₅₀, thus
21
22 identifying 4 chemical series. After data analysis, we have prioritized the chemical series of
23
24 N-phenyl-4H-thieno[3, 2-b]pyrrole-5-carboxamide for which we obtained X-ray structures of
25
26 the most potent hit (compound **19**, IC₅₀ = 2.9μM) in complex with the enzyme. Initial
27
28 expansion of this chemical class, both modifying core structure and decorating benzamide
29
30 moiety, was directed towards the definition of the moieties responsible for the interaction
31
32 with the enzyme. Preliminary optimization brought to compound **90** which inhibited the
33
34 enzyme with a submicromolar IC₅₀ (0.162μM), capable to inhibit the target in cells.
35
36
37

38 39 **INTRODUCTION**

40
41 Histone Lysine demethylases are responsible for post-translational modifications of the
42
43 histone tails,^{1,2} representing some of the most important partners in eukaryotic chromatin
44
45 regulation.³ Among them KDM1A (LSD1), homologous to polyamine oxidase (PAO) and
46
47 monoamine oxidase (MAO) A and B,⁴ catalyses mono- and dimethyl histone 3 lysine 4
48
49 (H3K4me1, H3K4me2) and H3K9 demethylation.⁴ High expression of KDM1A has been
50
51 reported in acute myeloid leukemia⁵, lymphoid neoplasm⁶, prostate cancer,⁷ ER-negative
52
53 breast cancer⁸ and neuroblastoma.⁹ Moreover its high expression correlates with poor
54
55 prognosis in several tumor types, such as breast cancer,⁷ prostate cancer,^{8, 10} non small cell
56
57
58
59
60

1
2
3 lung cancer¹¹ and hepatocellular carcinoma.¹² A role of KDM1A into conferring stem cell-
4
5 like characteristics in breast cancer has also been proposed.¹³
6

7 From the discovery of tranlycypromine (**1** in Figure 1) as an irreversible inhibitor of
8
9 KDM1A,^{14,15} a number of analogues bearing the cyclopropyl moiety has been described¹⁶⁻²⁰
10
11 and three clinical candidates are currently under investigation, two of them being disclosed,
12
13 ORY1001/RG-6016²¹ as compound **6** and GSK2879552^{22,23} as compound **7**, whereas
14
15 INCB059872 from Incyte is still structurally unknown.²⁴ We have also contributed to the
16
17 field with the recent identification of a potent oral selective inhibitor [(1S,2R)-**3**, Fig.1]²⁵ able
18
19 to significantly prolong survival time in a murine promyelocytic leukemia model.
20
21

22 Several examples of reversible KDM1A inhibitors have been reported in the literature (Fig.
23
24 **1**),^{16-20, 25-28} the development of which appears to be in the pre-clinical stage. A high-
25
26 throughput screening (HTS) using Time-resolved fluorescence energy transfer assay (TR-
27
28 FRET) on KDM1A has also been described, although no inhibitors were reported.²⁷ Here we
29
30 describe the identification of four chemical series that are active on KDM1A through the
31
32 screening of a representative subset of our chemical collection (ca. 34000 commercially
33
34 available compounds) and the process used to select the thieno[3,2-b]pyrrole-5-carboxamide
35
36 series for further development. A very preliminary exploration allowed us to obtain
37
38 submicromolar inhibitors. A subsequent extensive medicinal chemistry effort has led to a
39
40 further optimization of the series, up to the identification of highly selective nanomolar
41
42 inhibitors, endowed with high potency in cellular assays. This in depth exploration is the
43
44 subject of an accompanying paper.²⁸
45
46
47
48

49 **Insert Figure 1**

50 **RESULTS AND DISCUSSION**

51 **The Chemical Collection**

1
2
3 The starting point for any HTS activity is a proper compound collection. To perform HTS for
4
5 our projects, we built a structurally diverse collection, starting from five millions of
6
7 commercially available compounds, filtering out molecules on the basis of their physico-
8
9 chemical properties, removal of undesired features,^{29,30} diversity and chemotype
10
11 representativeness and we obtained a subset of 196,000 compounds, which were purchased.

12
13 This library was designed to represent each selected chemotype (scaffold-based) with a
14
15 sufficient number of close analogues to obtain preliminary SARs for each hit identified
16
17 during HTS. Although the chemical diversity is limited, the hit identification process is
18
19 reinforced with the reduction of false positive rate. The analogues would help in deciding if
20
21 positive (or negative) results are true values simply by looking at the whole activity range
22
23 across the cluster. At the same time the higher the number of cluster members (close
24
25 analogues), the lower the “chemical diversity”, independently from chemical diversity space
26
27 definition.

28
29 In order to maximize signal over noise ratio³¹, and to minimize the total number of assayed
30
31 compounds still maintaining high number of confirmed hits, the collection has been divided
32
33 into 5 subsets. Four of them, containing 8,500 chemical diversity representatives each, for a
34
35 total of 34,000, have been selected to be assayed in the first step of HTS. Close analogues of
36
37 hits are pooled from the fifth set (Full Diversity Set), represented by the remaining 162,000
38
39 compounds. These analogues are used during the hit expansion step. All compounds are
40
41 plated into 384 well plates, and are grouped by similarity, thus generating a sort of
42
43 “compound cartridges” ready for screening and allowing hit expansions with a minimal
44
45 effort.

52 **Quantitative High-Throughput Screening**

54 *Step 1*

1
2
3 The screening was conducted on 34000 compounds, the representative subset of our chemical
4 collection obtained from commercially available generic libraries, at the fixed concentration
5 of 10 μM (see Figure 2). The KDM1A inhibiting activity was determined using a TR-
6 FRET(time resolved fluorescence resonance energy transfer) assay. The assay was performed
7 at room temperature (RT) in 384 well plates in a final volume of 30 μL of assay buffer (Tris
8 HCl 50 mM pH 8.8, NaCl 50 mM, DTT 1 mM, Tween-20 0.01%, protease-free BSA 0.01%
9 w/v) at the enzyme (KDM1A/CoREST) and substrate (histone H3K4 monomethylated)
10 concentrations of 0.079 nM and 51 nM respectively. After 60 min at RT, the reaction was
11 stopped with tranlycypromine at the concentration of 300 μM . The primary screening
12 campaign was completed in 5 days and the assays provided an overall Robust z prime factor
13 (RZ') of 0.85, demonstrating the robustness and the quality of the obtained data. The
14 threshold for hit selection was set at 15% of activity, which corresponded to mean plus three
15 times the standard deviation computed on neutral controls (maximal signal in absence of
16 inhibitor). Compounds with high auto-fluorescence and therefore interfering with the assay
17 were discarded. Applying these criteria, 320 out of 34000 compounds were identified as hits,
18 corresponding to 0.95% hit rate. The 320 primary hits were then tested at 30 μM , 10 μM and
19 3 μM with inter-plate triplicates. 113 out of 320 retested compounds were confirmed with a
20 confirmation rate of 35 % and with an overall RZ' of 0.7. This result was consistent with the
21 threshold applied in primary screening for hit selection. Indeed, the majority of compounds
22 that did not confirm their activity were close to the primary screening threshold, whereas
23 most of the compounds showing high activity in primary screening, belonged to the group of
24 confirmed hits. Using these compounds as templates, substructure and similarity searches
25 against the fifth set of the collection was performed with ad hoc developed Pipeline Pilot³²
26 protocols. The protocols performed iteratively substructure and similarity searches (See
27 Experimental Section for details) for each of the reconfirmed hits and then collected and
28
29
30
31
32
33
34
35
36
37
38
39
40
41
42
43
44
45
46
47
48
49
50
51
52
53
54
55
56
57
58
59
60

1
2
3 merged all the results, thus producing a series of plates giving us the opportunity to screen an
4
5 enriched set of compounds similar to those obtained at 10 μ M.
6

7 8 *Step 2*

9
10 19 mother plates were selected from the Full Diversity set to be tested in triplicate at 10 μ M
11
12 to identify hits from analogous compounds present in the library. An overall RZ' of 0.81 was
13
14 obtained and 70 compounds among the 6080 tested were found to be active according to the
15
16 same threshold of the primary screening, thus producing a hit rate of 1.15% based on all
17
18 compounds and of 8% based on close analogs.
19

20 21 *Step 3*

22
23 Finally, a dose response experiment was conducted on 115 selected compounds. The
24
25 compounds were tested in dose-response at 8 concentrations ranging from 30 μ M to 0.1 μ M
26
27 with intra-plate quadruplicate data points. The overall RZ' was of 0.76 and 73 active
28
29 compounds were identified. Among them 27 compounds showed an IC₅₀ higher than 30
30
31 micromolar, 32 compounds showed an IC₅₀ between 10 and 30 micromolar and 14
32
33 compounds showed and IC₅₀ lower than 10 micromolar. Overall four chemical series and 14
34
35 singletons were identified (Table 1).
36
37

38 39 **Insert Figure 2**

40 41 **HTS Results**

42
43 The four main chemical series identified are reported in Table 1. They were evaluated on the
44
45 basis of novelty, preliminary SAR evidence, chemical feasibility and Structure Based Drug
46
47 Design (SBDD) amenability. Our interest was thus focused on compounds **19** and **21**.
48
49 Compound **19** (and its furo analogue) showed an interesting preliminary SAR having 20
50
51 analogues with IC₅₀ ranging from 10 to 30 micromolar. Compound **21**, although belonging to
52
53 a much smaller cluster, has a low molecular weight, comparable to a fragment, with a single
54
55
56
57
58
59
60

1
2
3 digit micromolar IC_{50} , and was considered for further investigation, taking into account its
4
5 high potential for derivatization.
6

7 **Insert Table 1**

8
9 The chemical series prioritized, thieno(furo)pyrroles **19** and spiro derivatives **21**, were
10
11 selected for further studies to better define their biochemical mechanism of action and to
12
13 verify their amenability for X-ray crystallography.
14

15 **Orthogonal assay, reversibility and selectivity**

16
17 Compounds **19**, **21** and tranylcypromine **1** were assessed with an orthogonal KDM1A assay
18
19 based on Horseradish Peroxidase (HRP) assay to reduce the probability to pursue false
20
21 positives and to obtain an independent confirmation of their histone demethylases activity. As
22
23 reported in Table 2, they inhibited KDM1A/CoREST complex also in the HRP assay
24
25 confirming to be genuine KDM1A inhibitors. Different experimental assay conditions in
26
27 terms of enzyme, substrate concentrations and incubation time used in the two assays justify
28
29 the differences between the TR-FRET and HRP reported IC_{50} s. Similar differences were
30
31 observed between HTS and reconfirmation data.
32
33
34
35

36 **Insert Table 2**

37
38 Since HRP assay is a continuous assay well suited to perform enzymatic inhibition kinetic
39
40 analysis, it was used to verify reversibility and biochemical mechanism of action of
41
42 compounds **19** and **21**. The reversibility was assayed by measuring the recovery of enzymatic
43
44 activity after a rapid and large dilution of the enzyme-inhibitor complex in presence of the
45
46 substrate. Consistently with its irreversible mechanism of action, incubation of **1** resulted in
47
48 complete inactivation of the enzyme, which was not recovered after dilution with the assay
49
50 buffer containing the substrate (Figure 3A). On the contrary, when KDM1A/CoREST was
51
52 incubated with **19** and **21**, the recovery of enzymatic activity after dilution was almost
53
54 complete, confirming for both compounds the reversibility of inhibition.
55
56
57
58
59
60

1
2
3 KDM1A/CoREST enzymatic kinetic was assessed at different concentrations of substrate and
4 inhibitor. Initial velocities were fitted to the equations for competitive, non-competitive and
5 uncompetitive inhibition, using SigmaPlot (Systat Software, San Jose, CA). As reported in
6
7 Figure 3B-C, Lineweaver-Burk plot indicates a non competitive mechanism for **19** and a
8 competitive mechanism for **21**. In particular **19** showed to be a non competitive type inhibitor
9 ($\alpha=1.1$)³³ with same affinity for free KDM1A/CoREST complex and the KDM1A/CoREST
10 enzyme substrate complex, with a K_i of 43 μM , whilst **21** showed to be a competitive
11 inhibitor, with a K_i of 48.4 μM .
12
13
14
15
16
17
18
19
20

21 **Insert Figure 3**

22
23 Finally, we investigated enzyme selectivity of **19** and **21** against KDM1B, MAOA and
24 MAOB using tranlycypromine **1** as reference. Both compounds showed high selectivity in the
25 secondary assay, as illustrated in Table 3.
26
27
28
29

30 **Insert Table 3**

31 **Structural analysis**

32
33 The N-[3-(methoxymethyl)phenyl]-4-methyl-thieno[3,2-b]pyrrole-5-carboxamide (**19**) was
34 successfully crystallized in complex with KDM1A/CoREST construct, see Materials and
35 Methods for details, and the X-ray diffraction quality allowed us to solve the complex at a
36 resolution of 3.2Å, adequate for structural analysis (see figure 4A and Table 1S in Supporting
37 Information). We also attempted to produce KDM1A/CoREST crystal in complex with
38 compound **21** but all the trials failed. To our knowledge **19** is the first small molecule in close
39 contact with FAD, reversibly inhibiting KDM1A, for which the experimentally determined
40 structure of the complex has been reported.
41
42
43
44
45
46
47
48
49
50

51 *Key interactions*

52
53 The ligand is located within the catalytic site of the KDM1A enzyme, as seen in Figure 4A,
54 with a relatively planar conformation due the electronic delocalization between the 2 ring
55
56
57
58
59
60

1
2
3 systems bridged by the amide group. The inhibitor interaction with the target is mainly
4 hydrophobic with no visible polar contacts. Its core, the thienopyrrole moiety, is caged
5 between residues Val333, Thr335, Leu663, Tyr765 and Thr814. The flavin ring represents
6 the back wall of such cage and the geometry of its contact with the bicyclic system is
7 compatible with an aromatic-aromatic interaction. The second ring system, an aryl group, is
8 packed between residues Val333, Phe542 and Trp699. The exit vector of the meta substituent
9 on the second ring system points toward Gln358, suggesting a possible interaction region.

10
11
12 Stability of the complex and its interactions have been evaluated using Molecular Dynamics
13 (MD) technique, propaedeutic to structure based drug design setup (see next paragraph).

14
15
16
17
18
19
20
21
22
23 Molecular details of the non-competitive inhibition mechanism for **19** are revealed by the
24 comparison of this crystallographic structure with the one of KDM1A in complex with
25 histone H3 peptide (2V1D)³⁴ depicted in figure 4B. The superposition of the two structures
26 shows a very partial overlap of the thienopyrrole molecule with the atoms of the peptide, only
27 the oxygen of the methoxymethyl superimpose with the histone, in a non effective manner. In
28 particular, the ligand is proximal to the region where the dimethylated lysine interacts with
29 the target to undergo the demethylation reaction.³⁵ Further comparison of the two KDM1A
30 complexes (2V1D vs internal) highlights subtle differences of binding-site residue
31 conformations. The two binding sites are quite identical with the exception of Trp699, which
32 is present with different rotamers. The different conformation of this amino acid is due to the
33 induced fit effect of thienopyrrole ligand binding to the target.

34 35 36 37 38 39 40 41 42 43 44 45 46 47 **Insert Figure 4**

48 49 50 **Structure Based Drug Design**

51
52 To support the development of this class of inhibitors, a specific molecular docking protocol
53 was developed to better reproduce the binding mode of the thienopyrrole chemotype. A
54 procedure was developed by combining docking programs, clustering techniques and energy
55
56
57
58
59
60

1
2
3 estimates (see Experimental Section for details). The KDM1A protein conformations used for
4
5 the docking procedures were those obtained from internal X-ray trials, where the
6
7 conformation of Trp699 has shifted with respect to its reported position. This effect is
8
9 induced by the binding of the ligand and in particular is due to the phenyl ring position
10
11 (Figure 4B). The use of these protein structures and the docking protocols gave satisfactory
12
13 results to reproduce the X-ray crystallographic conformation of **19** and produced reasonable
14
15 poses.
16
17

18
19 The conformational space of the ligand inside the target was explored with more than one
20
21 methodology: Autodock³⁶, Plants³⁷ and Glide³⁸ produced multiple docking poses. They were
22
23 clustered with the ACIAP (Autonomus-hierarchical clustering),³⁹ a method based on their
24
25 distances as RMSD between conformations. Finally, one representative pose per family was
26
27 submitted to BEAR (Binding estimation after refinement)⁴⁰ evaluation.
28

29
30 To identify binding site characteristics, such as hydrophobic-interaction pattern and hydrogen
31
32 bonding propensity, we chose to explore the target protein with a grid-based approach.
33
34 Autogrid software³⁶ was used to build different types of energetics maps applying various
35
36 atomic probes and the visualization of grid points below a certain threshold allowed us to
37
38 scan the binding site for favorable interaction regions. Of all obtained maps, the hydrophobic
39
40 pattern was quite informative and, associated to the electronegative areas, gave useful
41
42 suggestions for the development of the thienopyrrole series. As seen in Figure 5 the ligand is
43
44 buried into the hydrophobic region.
45
46

47 **Insert Figure 5**

48
49 The analysis of the electrostatics maps reveals two negatively charged regions, one in the
50
51 upward direction with respect to the thienopyrrole, where the residues Asp379 and Glu383
52
53 are found, and one downward, corresponding to residues Asp559, Asp560 and Glu563. In
54
55 particular, the former corresponds to the site where the guanidine group of the Arg8 of the
56
57
58
59
60

1
2
3 histone substrate interacts with the enzyme, see Figure 5B. Thus, we decided to grow the
4
5 chemical class elongating the substituent in position meta of the anilide in search of a
6
7 favorable interaction regions along the upward direction. In addition, the distance between
8
9 the benzene carbon in *para* position and the electronegative region is approximately 12
10
11 Angstroms. Ultimately these modeling suggestions prompted us to elongate the dimethylene
12
13 chain of compound **19** into a chain ending with a positively charged group.
14
15

16 Preliminary SAR from HTS

17
18 Preliminary SAR indications referred to compound **19** can be obtained directly from the HTS
19
20 data (Table 4): thienopyrrole bicyclic ring is favoured to the furopyrrole analogue (**19** vs **25**,
21
22 **22** vs **29**); *meta* substitution on phenyl ring results in more potent compounds than the *ortho*
23
24 analogues (**24** vs **31**, **22** vs **33**); amido nitrogen substitution with methyl is detrimental for
25
26 activity (**38** and **40**); electron donor groups are preferred to halogens or to electron
27
28 withdrawing groups.
29
30

31 Insert Table 4

32 Explorative SAR

33
34 A small chemical exploration to further investigate the series represented by compound **21**
35
36 has been performed, but none of the synthesized compound reported any inhibitory activity
37
38 (data not shown) and the explorative activity concluded. For thienopyrroles derivatives
39
40 instead we initiated a more comprehensive SAR study.
41
42
43

44
45 We approached the modification on four areas (see Figure 6):
46

47 A: Different heterocycles to replace thienopyrrole;

48
49 Small substituents on the thienopyrrole;

50 B: Different chains replacement of the N-methyl group of the thienopyrrole;

51
52 C: Isosters of the amido function;

53
54
55 D: Variations of the *meta* substituent of the phenyl group.
56
57
58
59
60

Insert Figure 6

As demonstrated by X-ray structure, A and B regions are involved in binding/interactions with flavin adenine dinucleotide (FAD), thus they have been explored together.

Region D is involved in induced fitting of Trp699 and carries the exit vector toward putative interactions with negatively charged region.

Region C has been explored as linker replacement.

Synthetic Chemistry

The appropriate heterocyclic aldehydes (**102a-l**) were converted into the azido derivatives (**103a-l**), by reaction with ethyl 2-azidoacetate and potassium ethylate in ethanol. Subsequent cyclization occurred by refluxing in xylene, providing **104a-l**, which reacted with methyl iodide and sodium hydride in DMF to give **105a-l**. Ester function could either be directly transformed into amide by reaction with aniline and LiHMDS in THF, or hydrolyzed to the acids as in **106c** in LiOH, which in turn reacted with aniline previous activation to acyl chloride with thionyl chloride (see Scheme 1).

Insert Scheme 1

Halogenation of thienopyrrole **23** was performed according to Scheme 2. Chlorination with N-chlorosuccinimide as reported⁴¹ went exclusively in position 6 on the pyrrole ring affording 6-chloro-4-methyl-N-phenyl-thieno[3,2-b]pyrrole-5-carboxamide (**56**) with 26% yield. Bromination with N-bromo succinimide has been reported on a similar substrate⁴², but in our case it gave an inseparable mixture of the major 2-bromo derivative **44** and the 6-bromo analogue **57**. Compound **44** was alternatively prepared according to Scheme 1, starting from 5-bromothiophene-2-carbaldehyde (**102i**).

NIS gave a mixture of 6-Iodo (**58**), 2-Iodo (**59**) and 2,6-diIodo (**60**). Fluorination of the thiophene in position 2 (**61**) was achieved with N-fluorobenzenesulfonimide (NFSI) using LDA as a base. Attempts with NFSI and butyllithium⁴¹ failed to give the desired product.

Insert Scheme 2

The synthesis of 6-methoxymethyl and 6-methyl thienopyrroles (**62** and **63** respectively) and the synthesis of 2- and 6-(dimethylaminomethyl) thienopyrroles (**64** and **65** respectively) are reported in Supporting Information.

Thienopyrrole **104a** was either treated with alkyl halide, benzyl chloride, or phenylsulphonyl chloride, in presence of NaH in DMF, to give the intermediates **105m–q**, or was treated with phenylboronic acid and Cu(OAc)₂ in pyridine, to give **105p**. Subsequent hydrolysis to **106m–r**, conversion into the corresponding acyl chloride by treatment with thionyl chloride, and reaction with the required amine, gave final amides **66–91**.

Insert Scheme 3

Compounds **92–94** and the anilines ArNH₂ in Scheme 3, when not commercially available, in particular those used to generate **90** and **91**, were prepared according to the procedures reported in Supporting Info.

A: 1_ Variation of the Heterocycle

In order to verify if the interaction with FAD in the binding pocket could be mimicked by other heterocycles, we replaced the bicycle ring with several other hetero aromatic systems. As illustrated in Table 5, only the regioisomer **45** resulted almost equipotent to **23**, furopyrrole **28** was more than three times less potent, whereas pyrrolothiazoles (**46** and **47**), pyrroloimidazoles (**48** and **50**), pyrrolopyrrole (**49**), pyrrolopyrazole (**51**), thienothiophene, thienoimidazole (**52**, **93**) or benzothiophene completely abolished the inhibitory activity.

Insert Table 5**A: 2_ Ring Substitution**

We approached a limited exploration on all the accessible positions of the bicyclic system (Table 6). None of the substitutions demonstrated the opportunity to decorate the core scaffold. Among the residues selected to substitute the pyrrolic nitrogen, only ethyl in

1
2
3 compound **66** improved potency of almost three times when compared to the methyl
4
5 analogue **23**, whilst the other chains were all detrimental for the activity (see 2-aminoethyl,
6
7 phenyl, phenylsulfonyl and benzyl in compounds **68-71**). The reason for this inactivity can be
8
9 explained by steric hindrance of substituents in position 4 of thienopyrrole moiety: anything
10
11 larger than ethyl group in fact goes toward residues Leu663, Tyr765, as suggested in
12
13 comments to Fig 6A. Analogously, the proximity of the enzyme wall to the ligand does not
14
15 allow any atom replacing hydrogens in position 2, 3 and 6 of the thienopyrrole, neither small
16
17 alkyls, nor halogens of various type (**44**, **53-56**, **58-65**).

20 21 **Insert Table 6**

22 23 **C: Amide replacement**

24
25 In search of new functional groups substituting the amide spacer, we made some isosteric
26
27 replacements (ester, reverse amide, oxime) without any activity improvement (data not
28
29 shown).

30 31 32 **D:1_Phenyl replacement**

33
34 The phenyl group was replaced by several nitrogen containing six member rings, as
35
36 illustrated in Table 7, such as pyridine (**72-74**) or pirimidine (**75-76**) but none of them
37
38 resulted to be more potent than the parent compound.

39 40 41 **Insert Table 7**

42 43 **D: 2_Benzamide *meta* substituted**

44
45 From the data obtained, we concluded that the benzamido moiety is the only portion allowing
46
47 substitution, without substantially abolishing the inhibitory activity. Keeping in mind that **19**
48
49 resulted among the most interesting derivatives, we investigated several replacements of the
50
51 methoxy methyl in *meta* position (see Table 8).

52
53
54 Halogens, methoxy groups, tertiary amines (**22-24**, **26**, **77**, **78**), did not influence much the
55
56 activity, being the chlorine substituted (**26**) the most active compound, whereas primary
57
58
59
60

1
2
3 amides and bromine analogue were highly detrimental as in **79** and **80** (see Table 8a).
4
5 Variation of methoxymethyl brought to the methylthiomethyl derivative **32** and
6
7 morpholinomethyl **82** being slightly more potent, removal of the terminal methyl as in **85**
8
9 worsen the activity of four fold, whereas phenoxyethyl **86** caused a complete abolishment
10
11 of inhibitory potency, which was partially recovered with a p-OH substitution **84** (see Table
12
13 8b). The introduction of a pyridine (Table 8c) linked to the phenyl by a -CH₂O- group (as in
14
15 **88**) or by -OCH₂- (as in **87**) brought to a slight improvement of the activity, whereas the 4-
16
17 pyridinol derivative (**89**) resulted less active.

18
19
20
21 When observing the whole series of derivatives, a tendency in potency improvement in
22
23 presence of longer chains carrying a distal basic nitrogen emerges. In support of this
24
25 hypothesis, we observed a clear improvement with derivatives **90** and **91**: in both derivatives
26
27 p-piperidinoxyphenoxy substituent was able to increase the potency down to a
28
29 submicromolar range (**90**: IC₅₀=0.162μM, **91**: IC₅₀=0.442μM, Table 8d). Docking
30
31 experiments of **90** have been performed using internal produced protein structure, but the
32
33 presence of two negatively charged regions allowed dual pose orientations. Although the
34
35 uniqueness of the pose could not be established, in both cases the activity improvement is
36
37 well justified by the interactions of the piperidine moiety with one aspartate residue (Asp555
38
39 or Asp375). In Figure 7 is reported one of the accessible orientations.
40
41
42

43 **Insert Table 8**

44
45 **Insert Figure 7**

46
47 To further characterize this chemical class, we analyzed the selectivity profile of the two
48
49 most potent compounds: **90** and **91** using **6** as positive control. As reported for the initial hit
50
51 **19**, they demonstrated a high selectivity for KDM1A.
52
53

54 **Insert Table 9**

1
2
3 Compounds **90** and **91** were evaluated in terms of KDM1A inhibitory activity in acute
4 myeloid leukemia cell line THP-1. This cell line is characterized by the MLL-AF9
5 translocation, and was selected in consideration of the experimental evidences demonstrating
6 the relevance of KDM1A in sustaining the oncogenic potential of MLL-AF9 leukemia stem
7 cells.⁴³
8
9

10
11
12
13
14 The absence of evident effect on global level of histone H3K4 methylation after genetic
15 ablation of KDM1A, both in cancer cells⁴⁴ and hematopoietic cells,⁴⁵ let us to deprioritize
16 this experimental read out for cellular KDM1A inhibition experiments.
17
18
19

20
21 We evaluated instead the compound effects on the expression level of two differentiation
22 markers: CD14 and CD11B (modulated by KDM1A down regulation as reported in
23 Supporting Information), considering that KDM1A inhibition induces differentiation of
24 human AML cells⁵. As reported in table 9, **90** and **91**, as well as **6**, induced an increase of
25 mRNA expression of CD14 and CD11B selected genes, similarly to KDM1A down-
26 regulation by short hairpin RNA(shRNA). These results demonstrate the compounds ability
27 to block KDM1A activity in cells and to induce differentiation of THP-1 cells. To
28 additionally characterize their effects on leukemia cells, cell cycle analysis and assessment of
29 apoptosis induction were performed in THP-1 cells. As reported in Supporting Information
30 (Figure S2) treatment for 72 hours at the dose of 1 μ M for **90** and **91** and at the dose of 0.5
31 μ M for **6** did not induce apoptosis and cell death consistently with the expected cytostatic
32 pro-differentiation mechanism, due to KDM1A inhibition in AML cells^{25,43}. Finally, the
33 anticolonogenic potential of **90** was determined in the human MLL-AF9 leukemia cell line
34 THP-1. As reported in the table 10, at dose of 5 μ M, **90** was able to inhibit the colony
35 formation in THP-1 cells. Moreover, **90** - as well as **6** - induces differentiation in THP-1 cells
36 as demonstrated by expression increases of CD86 in the cells - recovered at the end of
37 semisolid culture experiment.
38
39
40
41
42
43
44
45
46
47
48
49
50
51
52
53
54
55
56
57
58
59
60

CONCLUSIONS

We run an HTS (TR-FRET assay) on 34000 compounds, in search of reversible inhibitors of the demethylase KDM1A, identifying 4 chemical classes inhibiting the enzyme at a low micromolar concentration. We prioritized thieno[3,2-b]pyrrole-5-carboxamides and 3,8-diazaspiro[4.5]decanes, demonstrating the biochemical mechanism of action for each hit selected in both the series.

The binding mode of a representative compound of thienopyrrole series was experimentally determined through X-ray crystallography and represents the first structural knowledge of KDM1A reversible inhibitors. With this notion we expanded the class modifying the scaffold, the amido linker and the aryl on the benzamide moiety. We discovered that residues bearing a terminal basic moiety located at about 18 Å away from thienopyrrole centroid drastically improved the activity. Further SAR exploration of the chemical series is reported in part 2,²⁸ in which we approached the ambiguity of the binding poses.

EXPERIMENTAL SECTION

HTS Assay Conditions (KDM1A Enzyme Inhibition)

To identify small molecule reversible inhibitor of KDM1A enzyme, TR-FRET technology was used to follow KDM1A enzymatic activity. In our *assay* a biotinylated H3K4me1 peptide substrate underwent demethylation and the demethylated products were then captured by the Eu-labeled antibody (Eu-Ab) and U Light Streptavidin (U Light-SA), thus bringing the Eu donor and U Light acceptor dye molecules into close proximity.

Upon irradiation at 340 nm, the energy from the Eu donor is transferred to the U Light acceptor dye which, in turn, generates light at 665 nm. The intensity of the light emission is proportional to the level of biotinylated reaction product. Once identified the best configuration of the assay in 384 format, optimizing the reaction and the detection conditions, assay adaptation to the automated screening-compatible conditions was performed, including

1
2
3 the analysis of intra-day variability and the spatial uniformity assessment. The overall RZ'
4
5 mean for the day 1 and day 2 plates respectively of 0.79 and 0.89, indicated the robustness of
6
7 the identified conditions and protocol. Inter and intra-plate variability analysis identified no
8
9 issues, the variability observed being below the threshold of 20%. RZ' is defined as:

$$RZ' = 1 - [3RSD (NC) + 3RSD (IC)] / (|\langle NC \rangle - \langle IC \rangle|)$$

14 RSD = robust standard deviation;

15
16 $\langle \rangle$ = median of the signal values for the indicate control wells of a plate (NC for neutral
17
18 control, IC for Inhibitor control).
19

20
21 The KDM1A inhibiting activity was determined using a TR-FRET assay (time resolved
22
23 fluorescence resonance energy transfer, Lance[®] Ultra Demethylase technology, Perkin Elmer,
24
25 Waltham, MA, USA), which comprises a Europium chelate donor dye (TRF0404, Perkin
26
27 Elmer, Waltham, MA, USA) together with ULight[™] (TR0102, Perkin Elmer, Waltham, MA,
28
29 USA), a small molecular weight acceptor dye with a red-shifted fluorescent emission, and a
30
31 biotinylated 21 aminoacids histone H3-derived monomethylated peptide (H3K4me)
32
33 [Lys(Me1)4]-Histone H3 (1-21)-GGK(biotin), (64355, Anaspec, Fremont, CA, USA) as
34
35 substrate. The intensity of the light emission is proportional to the level of biotinylated
36
37 reaction product. The complex of human recombinant KDM1A/CoREST protein was
38
39 produced in *E. coli* as separate proteins and co-purified as previously described.^{46 34}
40
41

42
43 **Demethylase Assay conditions:** the enzymatic assay was performed in 384 well white plates
44
45 (6007290 OptiPlate[™], Perkin Elmer, Waltham, MA, USA) in a final volume of 30 μ L of
46
47 assay buffer (Tris HCl 50 mM pH 8.8, NaCl 50 mM, DTT 1 mM, Tween-20 0.01%, protease-
48
49 free BSA 0.01% w/v) as follows: 10 μ L of 237 nM KDM1A/CoREST protein were first
50
51 incubated 10 minutes at RT with 10 μ L of 3 fold concentrated compounds (pre-diluted in
52
53 assay buffer at 1.5% DMSO). The reaction was then started adding with 10 μ L of 150 nM
54
55 histone H3K4 monomethylated substrate. After 60 min at RT, the reaction was stopped with
56
57
58
59
60

1
2
3 10 μ L of 1.2 mM tranlycypromine (P8511-1G, Sigma-Aldrich, St. Louis, MO 63103).

4
5 **Detection step conditions:** 10 μ L of detection Mix containing 1 nM Eu-antibody and 4 nM
6
7 U-*Light*-Streptavidin in 1X Lance Detection Buffer (TRF0404, TR0102, CR97100, Perkin
8
9 Elmer, Waltham, MA, USA) were dispensed on 40 μ L stopped reaction. The resulting
10
11 mixture was incubated in the dark for 1 h at RT. Then, TR-FRET signal was read by a
12
13 fluorimeter (PHERAstar^{Plus}, BMG LABTECH GmbH, Germany) (Excitation 337 nm,
14
15 Emission 665 nm and 620 nm, delay time 100 μ s, window time 200 μ s). Compound activity
16
17 and IC₅₀ values in dose response experiments were calculated on TR-FRET signal at 665 nm
18
19 using Genedata Screener[®] 10 (Genedata, Basel, Switzerland).
20
21

22 23 **Routine Assay Conditions (KDM1A Enzyme Inhibition)**

24
25 **Demethylase Assay conditions:** 0.25 nM KDM1A/CoREST protein and compound in 100%
26
27 DMSO were added in a final volume of 48 μ L assay buffer (Tris HCl 50 mM pH 8.8, NaCl
28
29 50 mM, DTT 1 mM, Tween-20 0.01%) to each well of a 96 well half area flat bottom white
30
31 plate (3693 Costar, Sigma-Aldrich, St. Louis, M, USA).
32
33

34 Demethylase reaction was started by the addition of 50nM histone H3K4 monomethylated.
35
36 After 20 min at RT, 300 μ M tranlycypromine (P8511-1G, Sigma-Aldrich, St. Louis, MO
37
38 63103) was added to stop the reaction.
39
40

41 **Detection step conditions:** 10 μ L of the assay mixture was transferred from the original plate
42
43 into a 384 well white plate (6007290 OptiPlate[™], Perkin Elmer, Waltham, MA, USA) and
44
45 10 μ L of the detection Mix containing 2 nM Eu-antibody and 10 nM U-*Light*-Streptavidin in
46
47 1X Lance Detection Buffer (TRF0404, TR0102, CR97100, Perkin Elmer, Waltham, MA,
48
49 USA). The resulting mixture was incubated in the dark for 1 h at RT. Then, TR-FRET signal
50
51 was read by a fluorimeter (Infinite[®] F200, Tecan, Männedorf, Swizerland) (Excitation
52
53 320nm, Emission 665 nm and 620 nm, delay time 50 μ s, window time 100 μ s).
54
55

56 57 **Reversibility and Michaelis–Menten Analysis**

58
59
60

1
2
3 Biochemical characterization of reversibility and K_i was performed using the
4 KDM1A/CoREST Assay Horseradish Peroxidase. The complex of human recombinant
5 KDM1A/CoREST protein was produced in *Escherichia coli* as separate proteins and co-
6 purified. The experiments were performed in 96 well half area white plates (cat. 3693,
7 Corning, Corning, NY) using a mono-methylated H3-K4 peptide containing 21 amino acids
8 (custom synthesis done by Thermo Scientific) as substrate and in a in 40 μ l volume of 50 mM
9 TRIS-HCl, pH 8.0 and 0.05 mg/ml BSA buffer. The peptide purity was >95% as checked by
10 analytical high-pressure liquid chromatography and mass spectrometry. The demethylase
11 activity was estimated under aerobic conditions and at RT by measuring the release of H_2O_2
12 produced during the catalytic process by the Amplex[®] UltraRed detection system coupled
13 with horseradish peroxidase (HRP). Briefly, 20 nM of KDM1A/CoREST complex was
14 incubated at RT for 15 min in the absence and/or the presence of various concentrations of
15 the inhibitors, 50 μ M Amplex[®] UltraRed (Life Technologies) and 0.023 μ M HRP (Sigma) in
16 50 mM Tris-HCl pH 8.0 and 0.05 mg/ml BSA. The inhibitors were tested twice in duplicates
17 at each concentration. Tranylcypromine (Sigma) was used as control. After preincubation of
18 the enzyme with the inhibitor, the reaction was initiated by addition of 4.5 μ M of mono-
19 methylated H3-K4 peptide. The conversion of the Amplex[®] Ultra Red reagent to Amplex[®]
20 UltroxRed was monitored by fluorescence (excitation at 510 nm, emission at 595 nm) for
21 12 min and by using a microplate reader (Infinite 200, Tecan Group, Switzerland). Arbitrary
22 units were used to measure the level of H_2O_2 produced in the absence and/or in the presence
23 of inhibition. The maximum demethylase activity of KDM1A/CoREST was obtained in the
24 absence of inhibitors and corrected for background fluorescence in the absence of
25 KDM1A/CoREST. The IC_{50} was calculated using GraphPad Prism version 4.0 (GraphPad
26 Software, San Diego, CA).
27
28
29
30
31
32
33
34
35
36
37
38
39
40
41
42
43
44
45
46
47
48
49
50
51
52
53
54
55
56
57
58
59
60

1
2
3 **Reversibility** was determined using jump dilution. Specifically KDM1A/CoRest complex
4
5 was incubated at a concentration 100 fold over the concentration required for the enzymatic
6
7 activity with saturating concentrations of the inhibitor (10 fold of its biochemical IC₅₀). After
8
9 15 minutes of incubation, a 100-fold dilution into reaction buffer containing the H3K4me
10
11 substrate was then performed to initiate the reaction. The reaction progress curves were
12
13 followed and compared to a positive control (KDM1A/CoREST enzyme complex without
14
15 inhibitor). The irreversible inhibitor **1** was used as a control of irreversible inhibition.
16
17

18 **Michealis Menten analysis**

19
20 The K_i of compound **19** and **21** was determined using a Michaelis–Menten kinetic analysis
21
22 across multiple concentrations of both compounds. Initial velocities of biochemical assay
23
24 were then plotted toward substrate enzyme concentrations and fitted to the equations for
25
26 competitive, noncompetitive and uncompetitive inhibition, using SigmaPlot (Systat Software,
27
28 San Jose, CA)
29
30

31 **Bioluminescent-Coupled Assay for Monoamine oxidases (MAO-Glo Assay)**

32
33 The MAO Glo Assay from Promega (cat. V1402, Promega, Madison, WI) was used to
34
35 measure the effect of inhibitors on MAO A and MAO B activity. Human recombinant MAO
36
37 A and MAO B from SIGMA (M7316 and M7441) have been used for the screening The
38
39 assay was performed at RT in 50 μ L (25 μ L reaction solution + 25 μ L detection reagent) in
40
41 96 well half area white plates (cat. 3693, Corning, Corning, NY). Luminescence was
42
43 measured after 20 min incubation in the dark using a microplate reader (Infinite F200, Tecan
44
45 Group, Switzerland) with an integration time of 0.25 s per well. 16 ng/ μ L MAO A or
46
47 20ng/ μ L MAO B were incubated with different inhibitor concentrations (from 0.004 μ M to
48
49 100 μ M) for 15 min at RT in Promega MAO Buffer or Promega MAO B Buffer (MAO Glo
50
51 Assay kit, catalogue number V1402, Promega, Madison, WI). After 30 min of incubation the
52
53 reaction was stopped with the Promega detection reagent. All compounds were tested twice
54
55
56
57
58
59
60

1
2
3 and IC₅₀ values were calculated using GraphPad Prism version 4.0 (GraphPad Software, San
4
5 Diego, CA).
6

7 **Chemoinformatics**

8
9 To perform all chemoinformatics activities, including substructure searches, similarity
10 searches, clustering and to control all docking activities Pipeline Pilot (vesion 9.1) protocols
11 have been used; Clustering (as implemented in Pipeline Pilot component) and Similarity
12 Searches (similarity threshold between 0.85 and 9.0) have been performed using Tanimoto
13 distance and FCEP6 descriptors as implemented in Pipeline Pilot (BIOVIA).
14
15
16
17
18
19

20 Pipeline Pilot has been used also to verify absence of PAINS inhibitor features²⁹ in the
21 synthesized compounds, by means of SubStructureSearches (SSS) extracted from the PAINS
22 paper.
23
24
25
26

27 **Cellular Assay**

28 **Cell type**

29
30
31 Human leukemia THP-1 cells wer obtained from the Deutsche Sammlung von
32 Mikroorganismen und Zellkulturen and resulted to be mycoplasma free both by PCR and
33 Mycoalert (Lonza kit). Cells were grown in RPMI supplemented with 10% fetal bovine
34 serum, 2 mM l-glutamine, and antibiotics and maintained in a humidified tissue culture
35 incubator at 37 °C in 5% CO₂.
36
37
38
39
40
41
42

43 **Retroviral Constructs and Production of Retroviruses**

44
45 shRNA constructs were prepared in the MSCV-based pLMP retroviral vector. The hairpins
46 used in the study were #12 and #13 (scramble ShRNAs) and 1A#3 and 1A#5 (shRNAs
47 against KDM1A):
48
49

50
51 #12, AGTACGCGAAGAATACTATCGA
52

53 #13, AGTACGTTTCAGAATATCATCGAT
54

55
56 1A#3, AAGTGATACTGTGCTTGCCAC
57
58
59
60

1
2
3 1A#5, ATCTCAGAAGATGAGTATTATT
4

5 Supernatants from transfected Phoenix packaging cells were collected at 48 and 72 h after
6
7 transfection and immediately used for infections.
8

9 **Retroviral Transduction of THP-1 cells**

10 For THP-1 cells infection, cells were diluted in retroviral supernatants added with 8 µg/mL
11 polybrene and seeded at 10⁶ cells/well in 24-well plates. Spin infection was performed for 2
12 consecutive days (2 infections per day) at 1800 rpm for 45 min. Puromycin selection
13 (3µg/mL) started 24 h after the last cycle of infection. Assays were carried out 8 days after
14 beginning of infection.
15
16
17
18
19
20
21

22 **Immunoblots and Antibodies**

23 Whole cell extracts were obtained by lysis in SDS buffer (50 mM Tris-HCl, 10% glycerol,
24 2% SDS). Proteins were separated by SDS-PAGE, blotted onto PVDF membrane and probed
25 with the indicated antibodies. The antibodies used in the study were anti-LSD1(KDM1A)
26 (no. 2139, Cell Signaling), anti-KDM1B (Sigma HPA031269), and anti-HDAC1 (ab7028),
27
28
29
30
31
32
33

34 **Transcriptional assay**

35 Human acute myeloid leukemia THP-1 were grown in RPMI supplemented with 10% foetal
36 bovine serum, 2 mM l-glutamine, and antibiotics and maintained in a humidified tissue
37 culture incubator at 37 °C in 5% CO₂. Cells were treated at the fixed dose of 1 µM or with
38 vehicle (DMSO). After 24 h the cells were collected for RNA analysis. Total RNA was
39 purified using RNeasy Mini Kit (Qiagen, Valencia, CA), quantified and reverse transcribed.
40 mRNA levels were measured by quantitative RT-PCR (Fast SYBR Green Master mix,
41 Applied Biosystems Foster City, CA) using specific primers and normalized against TBP
42 mRNA. Results are presented as fold induction relative to vehicle treated cells (DMSO).
43
44
45
46
47
48
49
50
51
52
53
54 Primers used in this study were:

55
56 **CD14**, GTTCGGAAGACTTATCGACCA- ATCGTCCAGCTCACAAGGTT
57
58
59
60

1
2
3 **CD11B**, AACCCCTGGTTCACCTCCT- CATGACATAAGGTCAAGGCTGT

4
5 **TBP**, GCTGGCCCATAGTGATCTTT – CTTACACGCCAAGAAACAGT.

6 7 **Assessment of apoptosis by Annexin V and propidium iodide double staining**

8
9
10 Vehicle (DMSO) or drug-treated cells were stained with Annexin V and propidium iodide and
11 the percentages of apoptotic cells were determined by flow cytometry. Briefly, cells were
12 resuspended in annexin-V binding buffer (10mM Hepes pH 7.4, 150mM NaCl, 1mM MgCl₂,
13 3.6mM CaCl₂, 5mM KCl) containing 1/50 dilution of annexin-V-APC (eBioscience and 3ul
14 of PI (Sigma)-solution 50ug/ml in PBS. Cells were freshly analyzed using FACSCanto II
15
16
17
18
19
20
21 flow cytometers (BD Biosciences).

22 23 **Cell Cycle Analysis**

24
25 Cells were treated with vehicle (DMSO) or the reported inhibitors for 72 hours, then
26 harvested and fixed dropwise with 70% ethanol and kept at 4°C before analysis by flow
27 cytometry. Nucleic acids from fixed cells were stained with 1ml propidium iodide (50 ug
28 /mL) plus RNase A (Sigma) (250ug/mL), overnight at 4°C. DNA content was measured by
29
30
31
32
33
34
35
36
37 using FACSCanto II flow cytometers (BD Biosciences) analyzed using BD FACS Diva
38 Software and ModFit LT3.0.

38 39 **Cell Studies (Clonogenic Assay)**

40
41 For the clonogenic assay, THP-1 cells were plated at a density of 250 cells/plate and cultured
42 with drugs at reported doses in MethoCult H4435 Enriched (StemCell Technologies,
43 Vancouver, BC) according with the manufacturer instructions for 13 days. After this time,
44
45
46
47
48
49
50 colonies were counted. Percentage of inhibition is referenced versus the vehicle (DMSO)
51 treated cells.

52 53 **Crystallography**

54
55 Crystals of KDM1A/CoREST were obtained as described.⁴⁷ For structure determination of
56
57
58
59
60 enzyme-inhibitor complexes, crystals were soaked for 3-8 h in a solution consisting of 1.3 M

1
2
3 sodium/potassium tartrate, 100 mM N-(2-acetamido)-2-iminodiacetic acid pH 6.5, 12% (v/v)
4
5 glycerol, and 0.5e1 mM inhibitor. Diffraction data were measured at beamlines of the
6
7 European Synchrotron Radiation Facility (Grenoble, France) and the Swiss Light Source
8
9 (Villigen, Switzerland). Data processing and coordinate refinement were performed with
10
11 programs of the CCP4 package.⁴⁸
12
13

14 **Statistical Analysis**

15
16 SigmaPlot v11⁴⁹
17

18 **Protein preparation for docking**

19
20 The crystallographic coordinates of **19** were prepared as previously reported.⁵⁰ In summary,
21
22 the protein was added of hydrogen atoms in Chimera software, optimizing the H-bond
23
24 networking and minimizing their position with 1000 steps of Steepest Descent. Then with
25
26 Semiempirical Quantum Mechanics (SQM) first the hydrogen atoms were optimized till a
27
28 gradient norm of 50 and then the whole protein was fully optimized SQM for 50 steps. The
29
30 resulting structure was used to develop the inputs necessary for all modeling programs by
31
32 means of the procedure presented (BASH scripted) in the work.⁵⁰
33
34
35

36 **Favorable interaction regions**

37
38 Favorable interaction areas are derived from the exploration of proteins binding site with
39
40 various atoms as probes. This procedure maps the interaction energy between a probe, which
41
42 characterizes the type of interaction, and the target. Examples of the probes are aliphatic
43
44 carbon for the hydrophobic pattern or amine nitrogen for H-bond donor, etc. The Autogrid
45
46 facility (from Autodock software) is used for this grid-based energy evaluation. Thus, the
47
48 interaction is recorded placing the probe at each node of the grid in the binding site. Finally,
49
50 selecting the appropriate energy cut-off and displaying only the grid's points with energy
51
52 below such value, the favorable interactions are visualized.
53
54
55
56
57
58
59
60

1
2
3 The Autodock plugin⁵¹ for PyMOL software (The PyMOL Molecular Graphics System,
4 Version 1.7.4 Schrödinger, LLC.) reads these Autogrid files and generates the surface
5 representation on the graphical rendering of protein-ligand coordinates.
6
7

8 9 **Pose production**

10 To predict the putative binding pose of ligands interacting with the target a docking protocol
11 was used. In order to explore a larger portion of the conformational space for these
12 molecules, results from various docking programs were mixed together. The combination of
13 various methodologies has been previously observed to higher the chances of finding ligand
14 conformation close to the crystallographic structure and thus to enhance of docking
15 performances.³⁹ In our study, 3 programs were used: Autodock³⁶, Plants³⁷ and Glide³⁸ with
16 the settings described in our previous work.⁵⁰
17
18
19
20
21
22
23
24
25
26

27 **Pose clustering**

28 The docking predictions were processed as one ensemble undergoing cluster analysis to
29 reduce dataset dimensionality and to identify binding conformational families. The
30 methodology used for this step is ACIAP, Autonomous hierarchical agglomerative Cluster
31 Analysis based Protocol.³⁹ In brief, this method consists on the construction of a full
32 hierarchical tree of the predicted poses using the Root Mean Square Deviation (RMSD)
33 between ligand conformations as metric and the average linkage as criterion to determine the
34 distances. Finally, the clustering level to cut the tree is identified with the KGS penalty
35 function, which is based on the average spread of clusters at each tree level. The global
36 minimum of this function ensures the best compromise between the number of clusters and
37 the mean distances between clusters.
38
39
40
41
42
43
44
45
46
47
48
49
50

51 This methodology was implemented as automatic computational scripts by means of R
52 software⁵². Once the procedure is performed the medoid conformation for each cluster is kept
53 as the representative for the family of binding. In addition, the number of cluster members is
54
55
56
57
58
59
60

1
2
3 also used to judge the quality of a binding mode. The more a solution is found the more
4
5 probable it is.
6

7 **Pose scoring**

8
9 In our protocol, the surviving poses are then optimized and scored by means of BEAR⁴⁰
10 (binding estimate after refinement). With this method each docking solutions is minimized in
11 complex with the target for 2000 steps, then a 100 picoseconds Molecular Dynamics
12 simulation of sole ligand is run keeping frozen the protein. The resulting conformation of the
13 complex is re-minimized and scored (single point) with GBSA and PBSA. In addition to the
14 interaction energy estimation another value is used to judge the final pose: the RMSD value
15 of the ligand between the initial conformation and the one after the MD. The higher the
16 RMSD the less stable is the predicted conformation and thus the reliability of the binding
17 pose.
18
19
20
21
22
23
24
25
26
27
28

29 BEAR was implemented in house by means of Amber software package⁵³ and Chimera⁵⁴.
30
31

32 **Modeling protocols implementation**

33
34 Pose production, clustering and scoring were implemented within the architecture described
35 in our recent work.⁵⁰ The protocol was constructed in Pipeline Pilot³² with its usual
36 components plus the 'CADDD components' that we developed to use the modeling software
37 on a powerful GNU/Linux environment. This consists of PP sub protocols that invoke BASH
38 scripts via SSH calls. The scripts are a combination of command lines, to interface with the
39 wanted program, and scripting variables to automatize the process.
40
41
42
43
44
45
46

47 **Chemistry**

48 **General Procedures.**

49
50 Melting points were determined on a BUCHI Melting point B-540 and are uncorrected.
51
52 Reagents and solvents used, unless stated otherwise, were of commercially available reagent
53 grade quality and were used without further purification. Reaction solvents were used
54
55
56
57
58
59
60

1
2
3 anhydrous, purchased in Sure/Seal bottles stored over molecular sieves. Silica gel flash
4 chromatography purifications were performed on Merck silica gel 60 (0.04-0.063 mm) or
5
6
7 Biotage Isolera One system using pre-packed columns from Grace and Biotage. Nuclear
8
9
10 magnetic resonance spectra (^1H NMR) were recorded on a Agilent VNMRS 500 MHz
11
12 spectrometer at 300 K and are referenced in ppm (δ) relative to TMS. Coupling constants (J)
13
14 are expressed in hertz (Hz). HPLC-MS experiments were performed on an Acquity UPLC
15
16 apparatus, equipped with a diode array and a Micromass SQD single quadrupole (Waters). The
17
18 compounds used for biological tests were monitored at 220 and 254 nM, with two different
19
20 methods and their purity was found to be at least 95%. Semi-preparative HPLC was
21
22 performed on a Waters apparatus eluting the sample through a BEH C 18 column (5 μm ,
23
24 19mmx100mm) using decreasingly polar mixtures of water (containing 5% of MeCN and
25
26 0.1% of trifluoroacetic acid) and MeCN (containing 0.1% of trifluoroacetic acid).
27
28

29 30 **General procedure to prepare benzamido derivatives by direct amidation of esters**

31
32 3 mL (3 mmol) of a 1 M solution of LiHMDS in THF was added dropwise at 0°C to a stirred
33
34 solution of 1 mmol of ester and 1.25 mmol of the required aniline. The mixture was allowed
35
36 to spontaneously warm to rt then was poured into sat. NH_4Cl and extracted with DCM. The
37
38 combined organic layers were dried over Na_2SO_4 , filtered and evaporated and the oil residue
39
40 was purified by column chromatography (eluent: *n*-hexane/EtOAc, from 2% to 20% of
41
42 EtOAc) providing the desired compound.
43
44

45 Similarly prepared:

46
47 ***N*-(3-Methoxyphenyl)-4-methyl-thieno[3,2-*b*]pyrrole-5-carboxamide (22)** (from **105a** and
48
49 3-methoxyaniline): yield 40% (23 mg); pale brown solid; ^1H NMR (DMSO- d_6) δ (ppm): 9.96
50
51 (s, 1 H), 7.52 (d, $J=5.4$ Hz, 1 H), 7.45-7.41 (m, 1 H), 7.34-7.30 (m, 2 H), 7.26-7.19 (m, 2 H),
52
53 6.68-6.61 (m, 1 H), 4.01 (s, 3 H), 3.75 (s, 3 H); MS (ESI): m/z : 287 $[\text{M}+\text{H}]^+$.
54
55

56
57 **4-Methyl-*N*-phenyl-thieno[3,2-*b*]pyrrole-5-carboxamide (23)** (from **105a** and aniline):
58
59
60

1
2
3 yield 82% (100 mg); beige solid; pale yellow solid: $^1\text{H NMR}$ (CDCl_3) δ (ppm) 7.69 (br s, 1
4 H), 7.60 (m, 2 H), 7.38 (m, 2 H), 7.32 (d, $J= 5.4$ Hz, 1 H), 7.15 (m, 1 H), 6.99 (d, $J= 5.4$ Hz,
5 1 H), 6.95 (s, 1 H), 4.11 (s, 3 H); MS (ESI): m/z : 257 $[\text{M}+\text{H}]^+$.
6
7

8
9
10 **4-Methyl-N-phenyl-furo[3,2-b]pyrrole-5-carboxamide (28)** (from **105d** and aniline): yield
11 83% (65 mg); brown solid. $^1\text{H NMR}$ (CDCl_3) δ (ppm): 7.61-7.53 (m, 3 H), 7.51 (d, $J= 2.0$
12 Hz, 1 H), 7.40-7.33 (m, 2 H), 7.16-7.09 (m, 1 H), 6.60 (s, 1 H), 6.50 (d, $J= 2.0$ Hz, 1 H), 4.04
13 (s, 3 H); MS (ESI): m/z : 241 $[\text{M}+\text{H}]^+$.
14
15

16
17
18 **2-Bromo-4-Methyl-N-phenyl-thieno[3,2-b]pyrrole-5-carboxamide (44)** (from **105i** and
19 aniline): yield 78% (150 mg); beige solid. $^1\text{H NMR}$ (DMSO-d_6) δ (ppm): 10.05 (s, 1 H),
20 7.76-7.66 (m, 2 H), 7.59-7.52 (m, 1 H), 7.37-7.29 (m, 2 H), 7.28-7.22 (m, 1 H), 7.11-6.99 (m,
21 1 H), 3.97 (s, 3 H); MS (ESI): m/z : 336 $[\text{M}+\text{H}]^+$. Mp: 168-170 $^\circ\text{C}$
22
23
24

25
26
27 **6-Methyl-N-phenyl-thieno[2,3-b]pyrrole-5-carboxamide (45)** (from **105b** and aniline):
28 yield 38% (31 mg); yellow solid. $^1\text{H NMR}$ (CDCl_3) δ (ppm): 7.67 (br s, 1 H), 7.62-7.57 (m, 2
29 H), 7.42-7.35 (m, 2 H), 7.18-7.12 (m, 1 H), 7.04-7.00 (m, 1 H), 6.98-6.95 (m, 1 H), 6.93-6.91
30 (m, 1 H), 4.09 (s, 3 H); MS (ESI): m/z : 257 $[\text{M}+\text{H}]^+$. Mp: 145-148 $^\circ\text{C}$
31
32
33

34
35
36 **4-methyl-N-phenyl-pyrrolo[3,2-d]thiazole-5-carboxamide (46)** (from **105d** and aniline):
37 yield 8% (6 mg); white solid. $^1\text{H NMR}$ (CDCl_3) δ (ppm): 8.56 (s, 1 H), 7.74 (br. s., 1 H),
38 7.64 - 7.57 (m, 2 H), 7.44 - 7.34 (m, 2 H), 7.21 - 7.10 (m, 2 H), 4.15 (s, 3 H); MS (ESI): m/z :
39 258 $[\text{M}+\text{H}]^+$ Mp: 194-198 $^\circ\text{C}$
40
41
42

43
44
45 **4-methyl-N-phenyl-pyrrolo[2,3-d]thiazole-5-carboxamide (47)** (from **105e** and aniline):
46 yield 25% (3 mg); white solid. $^1\text{H NMR}$ (CDCl_3) δ (ppm): 8.71 (s, 1 H), 7.72 (br. s., 1 H),
47 7.64 - 7.57 (m, 2 H), 7.44 - 7.35 (m, 2 H), 7.20 - 7.13 (m, 1 H), 6.94 (s, 1 H), 4.25 (s, 3 H);
48 MS (ESI): m/z : 258 $[\text{M}+\text{H}]^+$. Mp: 150-154 $^\circ\text{C}$ dec.
49
50
51

52
53
54 **1,4-Dimethyl-N-phenyl-pyrrolo[2,3-d]imidazole-5-carboxamide (48)** (from **105f** and
55 aniline): yield= 49% (6 mg). $^1\text{H NMR}$ (CDCl_3) δ = 7.64-7.55 (m, 3 H), 7.50-7.45 (m, 1 H),
56
57
58
59
60

1
2
3 7.40-7.34 (m, $J = 7.8, 7.8$ Hz, 2 H), 7.16-7.10 (m, 1 H), 6.53 (s, 1 H), 4.09 (s, 3 H), 3.79 (s, 3
4 H); MS (ESI): m/z : 255 [M+H]⁺. Mp: 176-180 °C (dec 151°C)

7 **4-(Benzenesulfonyl)-*N*-phenyl-thieno[3,2-*b*]pyrrole-5-carboxamide (70)** (from **105q** and
8 aniline): yield 34% (35 mg). ¹H NMR (DMSO-*d*₆) δ (ppm): 7.12 (s, 1 H) 7.79-7.18 (m, 10 H)
9 8.13 (m, 2 H) 10.64 (s, 1 H); MS (ESI): m/z : 383 [M+H]⁺. Mp: 187-190 °C.

14 **4-Methyl-*N*-(3-pyridyl)thieno[3,2-*b*]pyrrole-5-carboxamide (72)** (from **105a** and pyridin-
15 3-amine): yield 30% (19 mg). ¹H NMR (DMSO-*d*₆) δ (ppm): 10.24 (s, 1 H), 8.93 (m, 1 H),
16 8.32-8.16 (m, 2 H), 7.55 (d, $J = 5.4$ Hz, 1 H), 7.42 (m, 1 H), 7.37 (s, 1 H), 7.26 (d, $J = 5.4$ Hz,
17 1 H), 4.03 (s, 3 H); MS (ESI): m/z : 258 [M+H]⁺. Mp: 161-164 °C.

23 **4-Methyl-*N*-(2-pyridyl)thieno[3,2-*b*]pyrrole-5-carboxamide (73)** (from **105a** and pyridin-
24 2-amine): yield 32% (52 mg). ¹H NMR (CDCl₃) δ (ppm): 8.57 (br s, 1 H), 8.35-8.29 (m, 2
25 H), 7.77 (m, 1 H), 7.35 (d, $J = 5.4$ Hz, 1 H), 7.10-7.05 (m, 2 H), 6.99 (d, $J = 5.4$ Hz, 1 H), 4.13
26 (s, 3 H); MS (ESI): m/z : 258 [M+H]⁺. Mp: 139-142 °C.

32 **4-Methyl-*N*-(4-pyridyl)thieno[3,2-*b*]pyrrole-5-carboxamide (74)** (from **105a** and pyridin-
33 4-amine): yield 34% (55 mg). ¹H NMR (CDCl₃) δ (ppm): 8.54 (m, 2 H), 7.90 (br s, 1 H),
34 7.60 (m, 2 H), 7.03 (s, 1 H), 7.37 (d, $J = 5.38$ Hz, 1 H), 6.99 (d, $J = 5.38$ Hz, 1 H), 4.12 (s, 3 H);
35 MS (ESI): m/z : 258 [M+H]⁺. Mp: 128-131 °C.

41 **4-Methyl-*N*-pyrimidin-2-yl-thieno[3,2-*b*]pyrrole-5-carboxamide (75)** (from **105a** and
42 pyrimidin-2-amine): yield 14% (8.9 mg). ¹H NMR (CDCl₃) δ (ppm): 8.68 (m, 2 H), 8.57 (br
43 s, 1 H), 7.37 (d, $J = 5.38$ Hz, 1 H), 7.08 (s, 1 H), 7.06 (m, 1 H), 6.99 (d, $J = 5.38$ Hz, 1 H), 4.15
44 (s, 3 H); MS (ESI): m/z : 259 [M+H]⁺. Mp: 175-177 °C.

50 **4-Methyl-*N*-pyrimidin-4-yl-thieno[3,2-*b*]pyrrole-5-carboxamide (76)** (from **105a** and
51 pyrimidin-4-amine): yield 18% (11 mg). ¹H NMR (CDCl₃) δ (ppm): 8.91 (m, 1 H), 8.66 (m, 1
52 H), 8.48 (br s, 1 H), 8.28 (dd, $J = 5.87, 0.98$ Hz, 1 H), 7.41 (d, $J = 5.38$ Hz, 1 H), 7.10 (s, 1 H),
53 6.99 (d, $J = 5.38$ Hz, 1 H), 4.13 (s, 3 H); MS (ESI): m/z : 259 [M+H]⁺.

1
2
3 ***N*-(3-Carbamoylphenyl)-4-methyl-thieno[3,2-*b*]pyrrole-5-carboxamide (79)** (from **105a**
4 and 3-aminobenzamide): yield 50% (71 mg); off-white solid. ¹H NMR (DMSO-*d*₆) δ (ppm):
5 10.11 (s, 1 H), 8.27-8.18 (m, 1 H), 7.94 (br s, 1 H), 7.89 (m, 1 H), 7.56 (m, 1 H), 7.53 (d,
6 *J*=5.49 Hz, 1 H), 7.44-7.30 (m, 3 H), 7.25 (d, *J*=5.49 Hz, 1 H), 4.03 (s, 3 H); MS (ESI): *m/z*:
7 300 [M+H]⁺.
8
9

10
11
12
13
14 ***N*-[3-(HydroxyMethyl)phenyl]-4-methyl-thieno[3,2-*b*]pyrrole-5-carboxamide (85)**

15
16 **105a** reacted with 3-[[*tert*-butyl(diMethyl)silyl]oxyMethyl]aniline. The thus formed amide
17 was purified by SCX cartridge dissolving the crude in MeOH:DCM 9:1 and eluting with 25
18 mL of MeOH:DCM 9:1. Purification procedure led to TBDMS protective group removal,
19 yielding **85** (31%, 30 mg). ¹H NMR (DMSO-*d*₆) δ (ppm): 9.96 (s, 1 H), 7.74 (m, 1 H), 7.60
20 (m, 1 H), 7.51 (d, *J*= 5.4 Hz, 1 H), 7.34 (s, 1 H), 7.29-7.21 (m, 2 H), 7.01 (m, 1 H), 5.20 (t,
21 *J*= 5.6 Hz, 1 H), 4.49 (d, *J*= 5.4 Hz, 2 H), 4.02 (s, 3 H); MS (ESI): *m/z*: 287 [M+H]⁺.
22
23
24
25
26
27
28

29
30 **4-Methyl-*N*-[3-(phenoxyMethyl)phenyl]thieno[3,2-*b*]pyrrole-5-carboxamide (86)** (from
31 **105a** and 3-(phenoxyMethyl)aniline, **86e** see Supporting Info). Yield 34% (25 mg); white
32 solid. ¹H NMR (DMSO-*d*₆) δ (ppm): 10.05 (s, 1 H), 7.86 (s, 1 H), 7.73-7.64 (m, 1 H), 7.52
33 (d, *J*= 5.4 Hz, 1 H), 7.37-7.27 (m, 4 H), 7.24 (d, *J*= 5.4 Hz, 1 H), 7.17-7.13 (m, 1 H), 7.04-
34 6.99 (m, 2 H), 6.96-6.91 (m, 1 H), 5.09 (s, 2 H), 4.01 (s, 3 H); MS (ESI): *m/z*: 363 [M+H]⁺.
35
36
37
38
39
40
41 Mp: 180-184 °C.
42

43 **General procedure to prepare benzamido derivatives via acyl chloride**

44
45 1.5 mmol of SOCl₂ and 2 drops of dry DMF were added at rt to a solution of 1 mmol of
46 carboxylic acid in 5 mL of dry DCM/THF. The mixture was stirred for 2 h under reflux. The
47 reaction mixture was then cooled down to rt and added to a solution of 1-1.5 mmol of aniline
48 in 7 mL of pyridine. The mixture was stirred for 30 min at rt and for further 45 min at 60 °C.
49
50
51
52
53
54
55
56
57
58
59
60 Then, the mixture was diluted with DCM, washed with a saturated NaHCO₃ solution and
brine, dried over Na₂SO₄, filtered and concentrated to give an oil which was purified by flash

1
2
3 column chromatography.

4
5 Similarly prepared:

6
7 **4-Methyl-N-phenyl-furo[3,2-b]pyrrole-5-carboxamide (28)** (from **106c** and aniline): yield
8
9 83% (65 mg); brown solid. ¹H NMR (CDCl₃) δ (ppm): 7.61-7.53 (m, 3 H), 7.51 (d, *J*= 2.0
10 Hz, 1 H), 7.40-7.33 (m, 2 H), 7.16-7.09 (m, 1 H), 6.60 (s, 1 H), 6.50 (d, *J*= 2.0 Hz, 1 H), 4.04
11 (s, 3 H); MS (ESI): *m/z*: 241 [M+H]⁺.
12
13

14
15 **1-Methyl-N-phenyl-4H-pyrrolo[2,3-d]imidazole-5-carboxamide (50)** (from **106f** and
16
17 aniline): yield 4% (7 mg). ¹H NMR (DMSO-d₆) δ (ppm): 11.47 (s, 1 H), 9.73 (s, 1 H), 7.80-
18
19 7.72 (m, 2 H), 7.68-7.62 (m, 1 H), 7.36-7.28 (m, 1 H), 7.08-6.99 (m, 2 H), 3.75 (s, 3 H); MS
20
21 (ESI): *m/z*: 241 [M+H]⁺.
22
23

24
25 **4-Ethyl-N-phenyl-thieno[3,2-b]pyrrole-5-carboxamide (66)** (from **106m** and aniline):
26
27 yield 90% (62 mg); beige powder. ¹H NMR (DMSO-d₆) δ (ppm): 10.00 (s, 1 H), 7.79-7.00
28
29 (m, 8 H), 4.58-4.46 (m, 2 H), 1.32 (t, *J*= 6.8 Hz, 3 H); MS (ESI): *m/z*: 271 [M+H]⁺.
30
31

32
33 **N-Phenyl-4-propyl-thieno[3,2-b]pyrrole-5-carboxamide (67)** (from **106n** and aniline):
34
35 yield 85% (69 mg); beige powder. ¹H NMR (DMSO-d₆) δ (ppm): 10.01 (s, 1 H), 7.82-6.97
36
37 (m, 8 H), 4.47 (t, *J*= 7.1 Hz, 2 H), 1.80-1.66 (m, 2 H), 0.81 (t, *J*= 7.6 Hz, 3 H); MS (ESI):
38
39 *m/z*: 285 [M+H]⁺.
40

41
42 **N,4-Diphenylthieno[3,2-b]pyrrole-5-carboxamide (68)** (from **106p** and aniline): yield 72%
43
44 (47 mg); beige powder. ¹H NMR (DMSO-d₆) δ (ppm): 10.24 (s, 1 H), 7.69-6.82 (m, 13 H);
45
46 MS (ESI): *m/z*: 319 [M+H]⁺.
47

48
49 **N-Phenyl-4H-thieno[3,2-b]pyrrole-5-carboxamide (69)** (from **106r** and aniline): yield 59%
50
51 (43 mg); ochre solid. ¹H NMR (DMSO-d₆) δ (ppm): 11.88 (s, 1 H), 9.94 (s, 1 H), 7.83-6.88
52
53 (m, 8 H); MS (ESI): *m/z*: 243 [M+H]⁺.
54

55
56 **4-Benzyl-N-phenyl-thieno[3,2-b]pyrrole-5-carboxamide (71)** (from **106o** and aniline):
57
58 yield 58% (45 mg); beige solid. ¹H NMR (DMSO-d₆) δ (ppm): 10.07 (s, 1 H), 7.75-6.95 (m,
59
60

1
2
3 13 H), 5.80 (s, 2 H); MS (ESI): m/z : 355 [M+Na]⁺. Mp: 168-170 °C.

4
5 **4-Methyl-*N*-[3-(4-methylpiperazin-1-yl)phenyl]thieno[3,2-*b*]pyrrole-5-carboxamide (77)**

6
7 (from **106a** and 3-(4-methylpiperazin-1-yl)aniline): yield 36% (38 mg); white solid. ¹H NMR
8
9 (DMSO-*d*₆) δ (ppm): 9.81 (s, 1 H), 7.51 (d, J = 5.4 Hz, 1 H), 7.40-7.36 (m, 1 H), 7.30 (s, 1
10
11 H), 7.24 (d, J = 5.4 Hz, 1 H), 7.21-7.18 (m, 1 H), 7.16-7.11 (m, 1 H), 6.68-6.64 (m, 1 H), 4.01
12
13 (s, 3 H), 3.18-3.03 (m, 4 H), 2.48-2.42 (m, 4 H), 2.22 (s, 3 H); MS (ESI): m/z : 355 [M+H]⁺.

14
15 ***N*-[3-(Dimethylamino)phenyl]-4-methyl-thieno[3,2-*b*]pyrrole-5-carboxamide (78)** (from

16
17 **106a** and N1,N1-dimethylbenzene-1,3-diamine): yield 27% (24 mg); light brown solid. ¹H
18
19 NMR (DMSO-*d*₆) δ (ppm): 9.78 (s, 1 H), 7.55-7.46 (m, 1 H), 7.30 (s, 1 H), 7.26-7.22 (m, 1
20
21 H), 7.17 (br s, 1 H), 7.10 (br s, 2 H), 6.50-6.42 (m, 1 H), 4.01 (s, 3 H), 2.89 (s, 6 H); MS
22
23 (ESI): m/z : 300 [M+H]⁺.

24
25 ***N*-[3-(3-Bromophenyl)-4-methyl-thieno[3,2-*b*]pyrrole-5-carboxamide (80)** (from **106a** and

26
27 3-bromoaniline): yield 35% (130 mg); white solid. ¹H NMR (DMSO-*d*₆) δ (ppm): 10.12 (s, 1
28
29 H), 8.11-8.03 (m, 1 H), 7.75-7.66 (m, 1 H), 7.57-7.50 (m, 1 H), 7.38-7.20 (m, 4 H), 4.01 (s, 3
30
31 H); MS (ESI): m/z : 336 [M+H]⁺. Mp: 153-157 °C.

32
33 **4-Methyl-*N*-[3-[(1-methyl-3-piperidyl)methoxy]phenyl]thieno[3,2-*b*]pyrrole-5-**

34
35 **carboxamide (81)** (from **106a** and 3-[(1-methyl-3-piperidyl)methoxy]aniline): yield 51% (58

36
37 mg); beige solid. ¹H NMR (DMSO-*d*₆) δ (ppm): 9.93 (s, 1 H), 7.52 (d, J = 5.4 Hz, 1 H), 7.46-
38
39 7.41 (m, 1 H), 7.33-7.28 (m, 2 H), 7.26-7.23 (m, 1 H), 7.23-7.18 (m, 1 H), 6.66-6.60 (m, 1
40
41 H), 4.01 (s, 3 H), 3.88-3.76 (m, 2 H), 2.86-2.75 (m, 1 H), 2.67-2.57 (m, 1 H), 2.15 (s, 3 H),
42
43 2.04-1.96 (m, 1 H), 1.95-1.86 (m, 1 H), 1.85-1.75 (m, 1 H), 1.75-1.59 (m, 2 H), 1.55-1.42 (m,
44
45 1 H), 1.14-0.99 (m, 1 H); MS (ESI): m/z : 384 [M+H]⁺.

46
47 ***N*-[3-[(Dimethylamino)methyl]phenyl]-4-methyl-thieno[3,2-*b*]pyrrole-5-carboxamide**

48
49 **(83)** (from **106a** and 3-[(dimethylamino)methyl]aniline, **83e** see Supporting Info): yield 30%

(31 mg); beige solid. ^1H NMR (DMSO- d_6) δ (ppm): 9.98 (s, 1 H), 7.84-6.88 (m, 7 H), 4.02 (s, 3 H), 3.54-3.35 (m, 2 H), 2.21 (br s, 6 H); MS (ESI): m/z : 312 [M-H].

***N*-[3-[(4-Hydroxyphenoxy)methyl]phenyl]-4-methyl-thieno[3,2-*b*]pyrrole-5-**

carboxamide (84) (from **106a** and 4-[(3-aminophenyl)methoxy]phenol, **84e** see Supporting Info): yield 52% (748 mg); pale brown solid. ^1H NMR (DMSO- d_6) δ (ppm): 10.04 (s, 1 H), 8.94 (s, 1 H), 7.83 (m, 1 H), 7.68 (m, 1 H), 7.52 (d, $J=5.4$ Hz, 1 H), 7.35-7.30 (m, 2 H), 7.24 (d, $J=5.4$ Hz, 1 H), 7.11 (m, 1 H), 6.85-6.80 (m, 2 H), 6.70-6.64 (m, 2 H), 4.98 (s, 2 H), 4.02 (s, 3 H); MS (ESI): m/z : 379 [M+H] $^+$.

4-Methyl-*N*-[3-(4-pyridylmethoxy)phenyl]thieno[3,2-*b*]pyrrole-5-carboxamide (87)

(from **106a** and 3-(4-pyridylmethoxy)aniline): yield 14% (15 mg); beige solid. ^1H NMR (DMSO- d_6) δ (ppm): 9.99 (s, 1 H), 8.62-8.54 (m, 2 H), 7.57-7.54 (m, 1 H), 7.52 (d, $J=5.4$ Hz, 1 H), 7.47-7.43 (m, 2 H), 7.35-7.30 (m, 2 H), 7.27-7.21 (m, 2 H), 6.75-6.70 (m, 1 H), 5.18 (s, 2 H), 4.01 (s, 3 H); MS (ESI): m/z : 364 [M+H] $^+$. Mp: 126-131 $^\circ\text{C}$.

4-Methyl-*N*-[3-(4-pyridyloxymethyl)phenyl]thieno[3,2-*b*]pyrrole-5-carboxamide (88)

(from **106a** and 3-(4-pyridyloxymethyl)aniline): yield 16% (17 mg); beige solid. ^1H NMR (DMSO- d_6) δ (ppm): 10.07 (s, 1 H), 7.76-7.71 (m, 2 H), 7.71-7.66 (m, 2 H), 7.52 (d, $J=5.4$ Hz, 1 H), 7.37-7.33 (m, 1 H), 7.31 (s, 1 H), 7.24 (d, $J=5.4$ Hz, 1 H), 7.01-6.97 (m, 1 H), 6.15-6.07 (m, 2 H), 5.08 (s, 2 H), 4.00 (s, 3 H); MS (ESI): m/z : 364 [M+H] $^+$. Mp: 295-298 $^\circ\text{C}$ dec.

4-Methyl-*N*-[3-(4-pyridyloxy)phenyl]thieno[3,2-*b*]pyrrole-5-carboxamide (89)

(from **106a** and 3-(4-pyridyloxy)aniline): yield 21% (22 mg); light brown solid. ^1H NMR (DMSO- d_6) δ (ppm): 10.25 (s, 1 H), 8.02-7.94 (m, 3 H), 7.78-7.72 (m, 1 H), 7.57-7.48 (m, 2 H), 7.37 (s, 1 H), 7.28-7.22 (m, 2 H), 6.29-6.20 (m, 2 H), 4.03 (s, 3 H); MS (ESI): m/z : 350 [M+H] $^+$.

4-Methyl-*N*-[3-[[4-(4-piperidyloxy)phenoxy]methyl]phenyl]thieno[3,2-*b*]pyrrole-5-

carboxamide (90) The reaction product between **106a** and tert-butyl 4-[4-[(3-

1
2
3 aminophenyl)methoxy]phenoxy]piperidine-1-carboxylate **90e** (see Supporting Info for
4 experimental details) was deprotected by acidic treatment, The reaction mixture was
5 concentrated *in vacuo*, a saturated aqueous solution of NaHCO₃ was added to the residue and
6 extracted with EtOAc. The combined organic phases were dried over Na₂SO₄ and
7 concentrated to yield **90** (53% over two steps, 57 mg) as a white solid. ¹H NMR (DMSO-d₆)
8 δ (ppm): 10.03 (s, 1 H), 7.90-7.79 (m, 1 H), 7.71-7.65 (m, 1 H), 7.52 (d, *J*= 5.4 Hz, 1 H),
9 7.36-7.30 (m, 2 H), 7.24 (d, *J*= 5.4 Hz, 1 H), 7.15-7.09 (m, 1 H), 6.95-6.83 (m, 4 H), 5.02 (s,
10 2 H), 4.28-4.17 (m, 1 H), 4.02 (s, 3 H), 2.97-2.87 (m, 2 H), 2.57-2.50 (m, 2 H), 1.92-1.79 (m,
11 2 H), 1.46-1.32 (m, 2 H); MS (ESI): *m/z*: 462 [M+H]⁺.

12
13
14
15
16
17
18
19
20
21
22
23 **4-Methyl-N-[3-[[4-[(1-methyl-4-piperidyl)oxy]phenoxy]methyl]phenyl]thieno[3,2-**
24 **b]pyrrole-5-carboxamide (91)** (from **106a** and 3-[[4-[(1-methyl-4-
25 piperidyl)oxy]phenoxy]methyl]aniline **91e**, see Supporting Info): yield 50% (67 mg); pale
26 pink solid. ¹H NMR (DMSO-d₆) δ (ppm): 10.03 (s, 1 H), 7.88-7.81 (m, 1 H), 7.72-7.65 (m, 1
27 H), 7.52 (d, *J*= 5.4 Hz, 1 H), 7.37-7.30 (m, 2 H), 7.24 (d, *J*= 5.4 Hz, 1 H), 7.15-7.10 (m, 1
28 H), 6.96-6.84 (m, 4 H), 5.02 (s, 2 H), 4.26-4.14 (m, 1 H), 4.01 (s, 3 H), 2.65-2.53 (m, 2 H),
29 2.21-2.06 (m, 5 H), 1.91-1.79 (m, 2 H), 1.65-1.50 (m, 2 H); MS (ESI): *m/z*: 476 [M+H]⁺. Mp:
30 152-154 °C.

41 **6-Chloro-4-methyl-N-phenyl-thieno[3,2-b]pyrrole-5-carboxamide (56)**

42
43 To a stirred solution of 0.05 g (0.2 mmol) of 4-methyl-N-phenyl-thieno[3,2-b]pyrrole-5-
44 carboxamide (**23**) dissolved in 4 mL of dry DCM, 0.027 g (0.21 mmol) of *N*-
45 chlorosuccinimide was added in 3 portions at 0 °C. The reaction mixture was allowed to
46 reach rt and stirred for about 17 h. The mixture was diluted with DCM (up to 30 mL) and
47 washed with saturated aqueous NH₄Cl solution (20 mL). The organic layer was dried over
48 Na₂SO₄, filtered and the solvent evaporated. The residue was purified by flash
49 chromatography (eluent *n*-hexane/EtOAc from 1% to 3% of EtOAc) to **56** (26%, 15 mg) as a
50
51
52
53
54
55
56
57
58
59
60

1
2
3 white solid. $^1\text{H NMR}$ (CDCl_3) δ (ppm): 8.47 (br s, 1 H), 7.65 (m, 2 H), 7.40 (m, 2 H), 7.34 (d,
4 $J=5.38$ Hz, 1 H), 7.17 m, 1 H), 6.98 (d, $J=5.38$ Hz, 1 H), 4.11 (s, 3 H); MS (ESI): m/z : 291
5
6 $[\text{M}+\text{H}]^+$. Mp: 161-165 °C.

7
8
9
10 **6-Iodo-4-methyl-*N*-phenyl-thieno[3,2-*b*]pyrrole-5-carboxamide (58)** **2-Iodo-4-methyl-*N*-**
11 **phenyl-thieno[3,2-*b*]pyrrole-5-carboxamide (59)** **2,6-Diiodo-4-methyl-*N*-phenyl-**
12 **thieno[3,2-*b*]pyrrole-5-carboxamide (60)**

13
14
15
16 To a stirred solution of 0.05 g (0.2 mmol) of 4-methyl-*N*-phenyl-thieno[3,2-*b*]pyrrole-5-
17 carboxamide (**23**) dissolved in 4 mL of dry DCM, 0.0274 g (0.20 mmol) of *N*-
18 iodosuccinimide was added in 3 portions at 0 °C. The reaction mixture was allowed to
19 reach rt and stirred for about 17 h. The mixture was diluted with DCM (up to 30 mL) and
20 washed with saturated aqueous NH_4Cl solution (20 mL). The organic layer was dried over
21 Na_2SO_4 , filtered and the solvent evaporated. The residue was purified by flash
22 chromatography (eluent *n*-hexane/EtOAc 8:2) and subsequently by preparative HPLC.

23
24
25
26
27
28
29
30
31
32 **58**: yield 18% (13 mg); off-white solid. $^1\text{H NMR}$ (CDCl_3) δ (ppm): 8.15 (br s, 1 H), 7.69 (m,
33 2 H), 7.41 (m, 2 H), 7.35 (d, $J= 5.4$ Hz, 1 H), 7.18 (m, 1 H), 7.09 (d, $J= 5.4$ Hz, 1 H), 4.11 (s,
34 3 H); MS (ESI): m/z : 383 $[\text{M}+\text{H}]^+$. Mp: 195-199 °C dec.

35
36
37
38
39
40
41
42
43
44
45
46 **59**: yield 16% (12 mg); off-white solid. $^1\text{H NMR}$ (CDCl_3) δ (ppm): 7.65 (br s, 1 H), 7.58 (m,
47 2 H), 7.38 (m, 2 H), 7.21 (s, 1 H), 7.16 (m, 1 H), 6.85 (s, 1 H), 4.06 (s, 3 H); MS (ESI): m/z :
48 383 $[\text{M}+\text{H}]^+$.

49
50
51
52
53
54
55
56
57
58
59
60 **60**: yield 2% (2 mg); off-white solid. $^1\text{H NMR}$ (CDCl_3) δ (ppm): 8.09 (br s, 1 H), 7.67 (m, 2
H), 7.41 (m, 2 H), 7.30 (s, 1 H), 7.19 (m, 1 H), 4.05 (s, 3 H); MS (ESI): m/z : 509 $[\text{M}+\text{H}]^+$.

2-Fluoro-4-methyl-*N*-phenyl-thieno[3,2-*b*]pyrrole-5-carboxamide (61)

0.47 mL (0.94 mmol) of a 2M solution of LDA in THF was added to a solution of 0.08 g
(0.3121 mmol) of 4-methyl-*N*-phenyl-thieno[3,2-*b*]pyrrole-5-carboxamide (**23**), in 2.3 mL of
dry THF at -78 °C. The mixture was stirred for 1 h, then a solution of 0.30 g (0.94 mmol) of

1
2
3 *N*-fluorobenzenesulfonimide in 1 mL dry THF was added. Stirring was continued at -78 °C
4
5 for 15 min. and at rt for 1 h. Water was added and the mixture extracted with EtOAc; the
6
7 organics were combined, dried over Na₂SO₄, filtered and evaporated to afford a brown oily
8
9 residue purified by flash chromatography (eluent *n*-hexane/EtOAc from 5% to 20% of
10
11 EtOAc). A further purification by preparative HPLC gave **61** (9%, 7.9 mg) as a white solid.
12
13 ¹H NMR (CDCl₃), δ (ppm): 7.63 (br s, 1 H), 7.58 (m, 2 H), 7.37 (m, 2 H), 7.15 (m, 1 H), 6.85
14
15 (s, 1 H), 6.55 (s, 1 H), 4.04 (s, 3 H); MS (ESI): *m/z*: 275 [M+H]⁺. Mp: 164-166 °C dec

18 **Synthesis of azido derivatives (103a-l)**

20 **Ethyl (Z)-2-azido-3-(2-thienyl)prop-2-enoate (103a)**

21
22 A solution of 0.3 g (2.7 mmol) of thiophene-2-carbaldehyde (**102a**) and 2.1 g (4.0 mmol) of
23
24 ethyl azidoacetate (25% in EtOH) was added dropwise to a solution of 1.4 g (4.0 mmol) of
25
26 KOEt in 6 mL of ethanol at 0 °C. The reaction mixture was stirred at 0 °C for 2 h and rt for
27
28 additional 2 h. The reaction mixture was poured into a saturated aqueous solution of NH₄Cl
29
30 and extracted with diethyl ether. The combined organics were dried (Na₂SO₄) and
31
32 concentrated in vacuo. The residue was purified by silica gel flash chromatography (eluent:
33
34 *n*-hexane/EtOAc, from 0% to 5% of EtOAc) to provide **103a** (33%, 200 mg) as a yellow
35
36 solid. ¹H NMR (CDCl₃) δ (ppm): 7.54-7.48 (m, 1 H), 7.37-7.31 (m, 1 H), 7.18 (s, 1 H), 7.12-
37
38 7.05 (m, 1 H), 4.43-4.30 (m, 2 H), 1.46-1.33 (m, 3 H).

39
40
41 Similarly prepared:

42
43
44 **Ethyl (Z)-2-azido-3-(3-thienyl)prop-2-enoate (103b)** (from **102b**): yield 25% (200 mg);
45
46 yellow oil. ¹H NMR (CDCl₃) δ (ppm): 7.93-7.86 (m, 1 H), 7.53-7.48 (m, 1 H), 7.37-7.31 (m,
47
48 1 H), 6.99-6.95 (m, 1 H), 4.45-4.29 (m, 2 H), 1.45-1.35 (m, 3 H).

49
50
51 **Ethyl (Z)-2-azido-3-(2-furyl)prop-2-enoate (103c)** (from **102c**): yield 39% (840 mg);
52
53 yellow solid. ¹H NMR (CDCl₃) δ (ppm): 7.53-7.47 (m, 1 H), 7.15-7.08 (m, 1 H), 6.88 (s, 1
54
55

1
2
3 H), 6.57-6.50 (m, 1 H), 4.36 (q, $J= 6.8$ Hz, 2 H), 1.39 (t, $J= 6.8$ Hz, 3 H); MS (ESI): m/z : 225
4
5 [M+H]⁺.
6

7 **Ethyl (Z)-2-azido-3-thiazol-4-yl-prop-2-enoate (103d)** (from **102d**): yield 29% (580 mg);
8
9 yellow solid. ¹H NMR (CDCl₃) δ (ppm): 8.86-8.75 (m, 1 H), 8.30-8.18 (m, 1 H), 7.34-7.19
10
11 (m, 1 H), 4.38 (q, $J= 6.8$ Hz, 2 H), 1.40 (t, $J= 6.8$ Hz, 3 H); MS (ESI): m/z : 225 [M+H]⁺.
12
13

14 **Ethyl (Z)-2-azido-3-thiazol-5-yl-prop-2-enoate (103e)** (from **102e**): yield 10% (200 mg);
15
16 yellow solid. ¹H NMR (CDCl₃) δ (ppm): 8.94-8.84 (m, 1 H), 8.13-8.03 (m, 1 H), 7.20 (s, 1
17
18 H), 4.39 (q, $J= 7.3$ Hz, 2 H), 1.42 (t, $J= 7.3$ Hz, 3 H); MS (ESI): m/z : 222 [M+H]⁺.
19
20

21 **Ethyl (Z)-2-azido-3-(3-methylimidazol-4-yl)prop-2-enoate (103f)** (from **102f**): yield 11%
22
23 (211 mg). ¹H NMR (CDCl₃) δ (ppm): 8.00-7.86 (m, 1 H), 7.57-7.49 (m, 1 H), 6.73 (s, 1 H),
24
25 4.41-4.35 (m, 2 H), 3.69 (s, 3 H), 1.45-1.35 (m, 3 H); MS (ESI): m/z : 225 [M+H]⁺.
26
27

28 **Ethyl (Z)-2-azido-3-(1-methylpyrrol-2-yl)prop-2-enoate (103g)** (from **102g**): the crude
29
30 was used in the next step without purification.
31

32 **Ethyl (Z)-2-azido-3-(2-methylpyrazol-3-yl)prop-2-enoate (103h)** (from **102h**): yield 15%
33
34 (151 mg); pale yellow solid. ¹H NMR (DMSO-d₆) δ (ppm): 7.57-7.41 (m, 1 H), 6.96 (d, $J=$
35
36 2.0 Hz, 1 H), 6.86 (s, 1 H), 4.32 (q, $J= 7.1$ Hz, 2 H), 3.89 (s, 3 H), 1.32 (t, $J= 7.1$ Hz, 3 H);
37
38 MS (ESI): m/z : 222 [M+H]⁺.
39
40

41 **Ethyl (Z)-2-azido-3-(5-bromo-2-thienyl)prop-2-enoate (103i)** (from **102i**): yield 28% (900
42
43 mg); orange oil. The crude was used in the next step without purification.
44

45 **Ethyl (Z)-2-azido-3-(5-methyl-2-thienyl)prop-2-enoate (103j)** (from **102j**): yield 31% (574
46
47 mg). ¹H NMR (CDCl₃) δ (ppm): 7.14 (d, $J= 3.4$ Hz, 1 H), 7.10 (s, 1 H), 6.74 (d, $J= 3.4$ Hz, 1
48
49 H), 4.36 (q, $J= 7.0$ Hz, 2 H), 2.54 (s, 3 H), 1.39 (t, $J= 7.1$ Hz, 3 H).
50
51

52 **Ethyl (Z)-2-azido-3-(4-methyl-2-thienyl)prop-2-enoate (103k)** (from **102k**): yield 95%
53
54 (630 mg); brown solid. ¹H NMR (DMSO-d₆) δ (ppm): 7.39 (s, 1 H), 7.37 (s, 1 H), 7.19 (s, 1
55
56
57
58
59
60

1
2
3 H), 4.29 (q, $J= 7.0$ Hz, 2 H), 2.20 (s, 3 H), 1.30 (t, $J= 7.1$ Hz, 3 H); MS (ESI): m/z : 210
4
5 [M+H]⁺.
6

7
8 **Ethyl (Z)-2-azido-3-(4,5-dimethyl-2-thienyl)prop-2-enoate (103l)** (from **102l**): yield 30%
9
10 (530 mg). ¹H NMR (DMSO-d₆) δ (ppm): 7.26 (s, 1 H), 7.12 (s, 1 H), 4.27 (q, $J= 7.3$ Hz, 2
11
12 H), 2.34 (s, 3 H), 2.07 (s, 3 H), 1.32-1.27 (m, 3 H).
13

14 **Synthesis of bicyclic rings (104a-l)**

15 **Ethyl 6H-thieno [2,3-b]pyrrole-5-carboxylate (104b)**

16
17 A solution of 0.18 g (0.81 mmol) of ethyl (Z)-2-azido-3-(3-thienyl)prop-2-enoate (**103b**) in 4
18
19 mL of xylene was heated at reflux for 30 min, concentrated in vacuo, diluted with diethyl
20
21 ether and then evaporated to dryness to give **104b** (96%, 151 mg) as a yellow solid. ¹H NMR
22
23 (CDCl₃) δ (ppm): 9.23 (br s, 1 H), 7.17-7.07 (m, 1 H), 7.05-6.98 (m, 1 H), 6.96-6.87 (m, 1
24
25 H), 4.44-4.27 (m, 2 H), 1.47-1.30 (m, 3 H); MS (ESI): m/z : 196 [M+H]⁺.
26
27
28

29 **Similarly prepared:**

30
31 **Ethyl 4H-thieno[3,2-b]pyrrole-5-carboxylate (104a)** (from **103a**): yield 91% (140 mg); red
32
33 solid. ¹H NMR (CDCl₃) δ (ppm): 9.07 (br s, 1 H), 7.37-7.30 (m, 1 H), 7.18-7.12 (m, 1 H),
34
35 7.00-6.94 (m, 1 H), 4.38 (q, $J= 6.8$ Hz, 2 H), 1.40 (t, $J= 6.8$ Hz, 3 H) MS (ESI): m/z : 196
36
37 [M+H]⁺.
38
39

40
41 **Ethyl 4H-furo[3,2-b]pyrrole-5-carboxylate (104c)** (from **103c**): yield 91% (655 mg);
42
43 yellow solid. ¹H NMR (DMSO-d₆) δ (ppm): 11.65 (br s, 1 H), 7.83-7.71 (m, 1 H), 6.77-6.68
44
45 (m, 1 H), 6.63-6.55 (m, 1 H), 4.25 (q, $J= 6.8$ Hz, 2 H), 1.28 (t, $J= 6.8$ Hz, 3 H); MS (ESI):
46
47 m/z : 180 [M+H]⁺.
48

49
50 **Ethyl 4H-pyrrolo [3,2-d]thiazole-5-carboxylate (104d)** (from **103d**): yield 99% (490 mg);
51
52 yellow solid. ¹H NMR (CDCl₃) δ (ppm): 9.30 (br s, 1 H), 8.57 (s, 1 H), 7.37-7.30 (m, 1 H),
53
54 4.40 (q, $J= 6.8$ Hz, 2 H), 1.41 (t, $J= 6.8$ Hz, 3 H); MS (ESI): m/z : 197 [M+H]⁺.
55

56
57 **Ethyl 4H-pyrrolo [2,3-d]thiazole-5-carboxylate (104e)** (from **103e**): yield 95% (150 mg);
58
59
60

1
2
3 yellow solid. ^1H NMR (CDCl_3) δ (ppm): 9.87 (br s, 1 H), 8.82-8.72 (m, 1 H), 7.20-7.10 (m, 1
4 H), 4.41 (q, $J=7.3$ Hz, 2 H), 1.42 (t, $J=7.3$ Hz, 3 H); MS (ESI): m/z : 197 $[\text{M}+\text{H}]^+$.

7 **Ethyl 1-methyl-4H-pyrrolo [2,3-d]imidazole-5-carboxylate (104f)** (from **103f**): yield 97%
8 (170 mg); brown solid. ^1H NMR (DMSO-d_6) δ (ppm): 11.63 (s, 1 H), 7.78-7.59 (m, 1 H),
9 6.70 (d, $J=1.5$ Hz, 1 H), 4.22 (q, $J=6.8$ Hz, 2 H), 3.71 (s, 3 H), 1.27 (t, $J=6.9$ Hz, 3 H);
10 MS (ESI): m/z : 194 $[\text{M}+\text{H}]^+$.

13 **Ethyl 1-methyl-4H-pyrrolo[3,2-b]pyrrole-5-carboxylate (104g)** (from **103g**): yield 54%
14 (190 mg), white solid. ^1H NMR (CDCl_3) δ (ppm): 8.41 (br. s, 1 H), 6.83-6.79 (m, 1 H), 6.77-
15 6.72 (m, 1 H), 5.97-5.91 (m, 1 H), 4.35 (q, $J=7.2$ Hz, 2 H), 3.70 (s, 3 H), 1.38 (t, $J=7.2$ Hz,
16 3 H); MS (ESI): m/z : 193 $[\text{M}+\text{H}]^+$.

19 **Ethyl 1-methyl-6H-pyrrolo [2,3-c]pyrazole-5-carboxylate (104h)** (from **103h**): yield 18%
20 (45 mg); white solid. ^1H NMR (DMSO-d_6) δ (ppm): 11.73 (br. s, 1 H), 7.44 (s, 1 H), 6.74 (s,
21 1 H), 4.26 (q, $J=7.3$ Hz, 2 H), 3.84 (s, 3 H), 1.29 (t, $J=7.3$ Hz, 3 H)

24 **Ethyl 2-bromo-4H-thieno[3,2-b]pyrrole-5-carboxylate (104i)** (from **103i**): yield 98% (800
25 mg); orange solid. ^1H NMR (DMSO-d_6) δ (ppm): 12.27-12.10 (m, 1 H), 7.18 (s, 1 H), 7.05
26 (s, 1 H), 4.33-4.18 (m, 2 H), 1.38-1.20 (m, 3 H); MS (ESI): m/z : 272 $[\text{M}-\text{H}]$

29 **Ethyl 2-methyl-4H-thieno[3,2-b]pyrrole-5-carboxylate (104j)** (from **103j**): yield 100%
30 (495 mg); orange solid. ^1H NMR (CDCl_3) δ (ppm): 8.89 (br s, 1 H), 7.06 (d, $J=1.5$ Hz, 1 H),
31 6.66 (s, 1 H), 4.36 (q, $J=7.0$ Hz, 2 H), 2.56 (s, 3 H), 1.39 (t, $J=7.1$ Hz, 3 H); MS (ESI): m/z :
32 210 $[\text{M}+\text{H}]^+$.

35 **Ethyl 3-methyl-4H-thieno[3,2-b]pyrrole-5-carboxylate (104k)** (from **103k**): yield 96%
36 (630 mg); brown solid. ^1H NMR (DMSO-d_6) δ (ppm): 12.12 (br s, 1 H), 7.09 (d, $J=1.0$ Hz,
37 1 H), 7.04 (d, $J=2.0$ Hz, 1 H), 4.28 (q, $J=7.3$ Hz, 2 H), 2.29 (d, $J=1.0$ Hz, 3 H), 1.30 (t, $J=$
38 7.1 Hz, 3 H); MS (ESI): m/z : 210 $[\text{M}+\text{H}]^+$.

41 **Ethyl 2,3-dimethyl-4H-thieno[3,2-b]pyrrole-5-carboxylate (104l)** (from **103l**): yield 96%

(426 mg). ^1H NMR (DMSO- d_6) δ (ppm): 11.97 (br s, 1 H), 6.97 (d, $J= 2.0$ Hz, 1 H), 4.26 (q, $J= 7.3$ Hz, 2 H), 2.35 (s, 3 H), 2.19 (s, 3 H), 1.29 (t, $J= 7.1$ Hz, 3 H); MS (ESI): m/z : 224 $[\text{M}+\text{H}]^+$.

Synthesis of substituted pyrrolic Nitrogen 105a-o, 105q

Ethyl 4-methylthieno[3,2-b]pyrrole-5-carboxylate (105a)

To a stirred suspension of 0.040 g (1.0 mmol) of NaH in 10 mL dry DMF, 0.130 g (0.67 mmol) of ethyl 4H-thieno[3,2-b]pyrrole-5-carboxylate (**104a**) was added portionwise over 5-10 min. The mixture was stirred 15 min at rt then 0.125 mL (2 mmol) of methyl iodide were added in one portion. After 1 h a solution of 10% NH_4Cl was added and the mixture extracted with diethyl ether. The organic phase was dried (Na_2SO_4), filtered and evaporated to give **105a** (99%; 138 mg) as a red oil. ^1H NMR (CDCl_3) δ (ppm): 7.34 (d, $J= 5.4$ Hz, 1 H), 7.20 (s, 1 H), 6.95 (d, $J= 5.4$ Hz, 1 H), 4.34 (q, $J= 7.3$ Hz, 2 H), 4.07 (s, 3 H), 1.39 (t, $J= 7.3$ Hz, 3 H); MS (ESI): m/z : 210 $[\text{M}+\text{H}]^+$.

Similarly prepared:

Ethyl 6-methylthieno [2,3-b]pyrrole-5-carboxylate (105b) (from **104b**): yield 98% (142 mg); yellow solid. ^1H NMR (CDCl_3) δ (ppm): 7.17 (s, 1 H), 7.00 (d, $J= 5.4$ Hz, 1 H), 6.93 (d, $J= 5.4$ Hz, 1 H), 4.34 (q, $J= 7.0$ Hz, 2 H), 4.04 (s, 3 H), 1.39 (t, $J= 7.1$ Hz, 3 H); MS (ESI): m/z : 210 $[\text{M}+\text{H}]^+$.

Ethyl 4-methylfuro[3,2-b]pyrrole-5-carboxylate (105c) (from **104c**): yield 99% (450 mg); red oil. ^1H NMR (CDCl_3) δ (ppm): 7.51 (d, $J= 2.4$ Hz, 1 H), 6.81 (s, 1 H), 6.45 (d, $J= 2.4$ Hz, 1 H), 4.31 (q, $J= 7.3$ Hz, 2 H), 3.98 (s, 3 H), 1.38 (t, $J= 7.3$ Hz, 3 H); MS (ESI): m/z : 194 $[\text{M}+\text{H}]^+$.

Ethyl 4-methylpyrrolo [3,2-d]thiazole-5-carboxylate (105d) (from **104d**): yield 98% (157 mg); yellow solid. ^1H NMR (CDCl_3) δ (ppm): 8.54 (s, 1 H), 7.36 (s, 1 H), 4.35 (q, $J= 7.0$ Hz, 2 H), 4.10 (s, 3 H), 1.40 (t, $J= 7.0$ Hz, 3 H); MS (ESI): m/z : 211 $[\text{M}+\text{H}]^+$.

Ethyl 4-methylpyrrolo [2,3-d]thiazole-5-carboxylate (105e) (from **104e**): yield 61% (13 mg); yellow solid. 61%. $^1\text{H NMR}$ (CDCl_3) δ (ppm): 8.72 (s, 1 H), 7.19 (s, 1 H), 4.37 (q, $J=7.3$ Hz, 2 H), 4.20 (s, 3 H), 1.44-1.35 (m, 3 H); MS (ESI): m/z : 211 $[\text{M}+\text{H}]^+$.

Ethyl 1,4-dimethylpyrrolo [2,3-d]imidazole-5-carboxylate (105f) (from **104f**): yield 51% (11 mg). $^1\text{H NMR}$ (CDCl_3) δ (ppm): 7.53-7.42 (m, 1 H), 6.84-6.72 (m, 1 H), 4.32 (q, $J=7.2$ Hz, 2 H), 4.03 (s, 3 H), 3.75 (s, 3 H), 1.38 (t, $J=7.2$ Hz, 3 H); MS (ESI) m/z : 208 $[\text{M}+\text{H}]^+$.

Ethyl 1,4-dimethylpyrrolo[3,2-b]pyrrole-5-carboxylate (105g) (from **104g**): yield 100% (107 mg); yellow solid. $^1\text{H NMR}$ (CDCl_3) δ (ppm): 6.83-6.79 (m, 1 H), 6.77 (s, 1 H), 5.95-5.88 (m, 1 H), 4.31 (q, $J=7.0$ Hz, 2 H), 3.96 (s, 3 H), 3.67 (s, 3 H), 1.38 (t, $J=7.0$ Hz, 3 H); MS (ESI): m/z : 207 $[\text{M}+\text{H}]^+$.

Ethyl 1,6-dimethylpyrrolo [2,3-c]pyrazole-5-carboxylate (105h) (from **104h**): yield 98% (45 mg); white solid. $^1\text{H NMR}$ (DMSO-d_6) δ (ppm): 7.44 (s, 1 H), 6.84 (s, 1 H), 4.23 (q, $J=7.3$ Hz, 2 H), 4.03 (s, 3 H), 4.00 (s, 3 H), 1.28 (t, $J=7.3$ Hz, 3 H); MS (ESI): m/z : 208 $[\text{M}+\text{H}]^+$.

Ethyl 2-bromo-4-methyl-thieno[3,2-b]pyrrole-5-carboxylate (105i) (from **104i**): yield 81%, (340 mg); light yellow solid. $^1\text{H NMR}$ (DMSO-d_6) δ (ppm): 7.56 (s, 1 H), 7.12 (s, 1 H), 4.25 (q, $J=7.3$ Hz, 2 H), 3.96 (s, 3 H), 1.29 (t, $J=7.1$ Hz, 3 H); MS (ESI): m/z : 288 $[\text{M}+\text{H}]^+$.

Ethyl 2,4-dimethylthieno[3,2-b]pyrrole-5-carboxylate (105j) (from **104j**): yield 70% (362 mg); pale yellow solid. $^1\text{H NMR}$ (CDCl_3) δ (ppm): 7.11 (s, 1 H), 6.64 (s, 1 H), 4.32 (q, $J=7.3$ Hz, 2 H), 4.01 (s, 3 H), 2.57 (d, $J=1.0$ Hz, 3 H), 1.38 (t, $J=7.3$ Hz, 3 H); MS (ESI): m/z : 224 $[\text{M}+\text{H}]^+$.

Ethyl 3,4-dimethylthieno[3,2-b]pyrrole-5-carboxylate (105k) (from **104k**): yield 74% (325 mg). $^1\text{H NMR}$ (CDCl_3) δ (ppm): 7.15 (s, 1 H), 6.89 (s, 1 H), 4.33 (q, $J=6.8$ Hz, 2 H), 4.21 (s, 3 H), 2.51 (s, 3 H), 1.38 (t, $J=7.3$ Hz, 3 H); MS (ESI): m/z : 224 $[\text{M}+\text{H}]^+$.

Ethyl 2,3,4-trimethylthieno[3,2-b]pyrrole-5-carboxylate (105l) (from **104l**): yield 49%

(218 mg). $^1\text{H NMR}$ (CDCl_3) δ (ppm): 7.08 (s, 1 H), 4.31 (q, $J=6.8$ Hz, 2 H), 4.20 (s, 3 H), 2.42 (s, 3 H), 2.39 (s, 3 H), 1.37 (t, $J=7.1$ Hz, 3 H); MS (ESI): m/z : 238 $[\text{M}+\text{H}]^+$.

Ethyl 4-Ethylthieno[3,2-b]pyrrole-5-carboxylate (105m) (from **104a** and ethyl iodide): yield 96% (1.1g); brown oil. $^1\text{H NMR}$ (CDCl_3) δ (ppm): 7.34 (d, $J=5.4$ Hz, 1 H), 7.20 (s, 1 H), 6.96 (d, $J=5.4$ Hz, 1 H), 4.56 (q, $J=7.3$ Hz, 2 H), 4.34 (q, $J=7.3$ Hz, 2 H), 1.46–1.34 (m, 6 H); MS (ESI): m/z : 224 $[\text{M}+\text{H}]^+$.

Ethyl 4-propylthieno[3,2-b]pyrrole-5-carboxylate (105n) (from **104a** and propyl bromide): yield 79% (240 mg); yellow oil. $^1\text{H NMR}$ (CDCl_3) δ (ppm): 7.37-7.29 (m, 1 H), 7.24-7.15 (m, 1 H), 6.99-6.90 (m, 1 H), 4.51-4.41 (m, 2 H), 4.38-4.28 (m, 2 H), 1.90-1.79 (m, 2 H), 1.44-1.32 (m, 3 H), 0.96-0.87 (m, 3 H); MS (ESI): m/z : 238 $[\text{M}+\text{H}]^+$.

Ethyl 4-benzylthieno[3,2-b]pyrrole-5-carboxylate (105o) (from **104a** and benzyl bromide): yield 84% (222 mg); yellow oil. $^1\text{H NMR}$ (CDCl_3) δ (ppm): 7.36-7.06 (m, 7 H), 6.90-6.78 (m, 1 H), 5.77 (s, 2 H), 4.30 (q, $J=7.0$ Hz, 2 H), 1.34 (t, $J=7.1$ Hz, 3 H); MS (ESI): m/z : 286 $[\text{M}+\text{H}]^+$.

Ethyl 4-(benzenesulfonyl)thieno[3,2-b]pyrrole-5-carboxylate (105q) (from **104a** and benzenesulfonyl chloride): yield 93% (160 mg); beige solid. $^1\text{H NMR}$ (DMSO-d_6) δ (ppm): 8.05-7.47 (m, 8 H), 4.21 (q, $J=7.3$ Hz, 2 H), 1.21 (t, $J=7.1$ Hz, 3 H); MS (ESI): m/z : 358 $[\text{M}+\text{Na}]^+$.

Ethyl 4-phenylthieno[3,2-b]pyrrole-5-carboxylate (105p)

4 mL of dry DCM, 0.143 mL (1.0 mmol) of triethylamine, 0.0825 mL (1.0 mmol) of pyridine and 0.5g of grounded 3A molecular sieves were added to 0.1 g (0.51mmol) of ethyl 4H-thieno[3,2-b]pyrrole-5-carboxylate (**104a**), 0.186 g (1.0 mmol) of $\text{Cu}(\text{OAc})_2$ and 0.125 g (1.0 mmol) of phenylboronic acid, under nitrogen atm. The mixture was vigorously stirred at rt for about 30 h and filtered through Celite, washed with DCM and EtOAc. The crude was purified by flash chromatography (eluent *n*-hexane:EtOAc from 1% to 10% of EtOAc) to

1
2
3 give **105p** (97%, 135 mg) as a beige solid. ^1H NMR (CDCl_3) δ (ppm): 7.56-7.19 (m, 7 H),
4 6.84-6.60 (m, 1 H), 4.21 (q, $J= 7.3$ Hz, 2 H), 1.26-1.18 (m, 3 H); MS (ESI): m/z : 272
5
6
7 [M+H] $^+$.
8

9
10 **Synthesis of carboxylic acids (106a, 106c, 106f, 106m-p, 106r)**

11
12 **4-methylfuro[3,2-b]pyrrole-5-carboxylic acid (106c)**

13
14 0.365 g (2.2 mmol) of LiOH in 5 mL of H_2O was added at rt to a solution of 0.45 g (2.33
15 mmol) of ethyl 4-methylfuro[3,2-b]pyrrole-5-carboxylate (**105c**) in 5 mL of ethanol, and the
16 mixture was heated to reflux for about 1 h. Ethanol was evaporated, water was added and the
17 pH brought to about 2 with 2 M HCl. The formed solid was filtered, washed with water and
18 dried to give **106c**, (95%, 365 mg) as beige solid. ^1H NMR (METHANOL- d_4) δ (ppm): 7.60
19 (d, $J= 2.2$ Hz, 1 H), 6.77 (s, 1 H), 6.60 (d, $J= 2.2$ Hz, 1 H), 3.96 (s, 3 H); MS (ESI): m/z : 166
20
21 [M+H] $^+$.
22
23
24
25
26
27
28

29 Similarly prepared:

30
31
32 **4-Methylthieno[3,2-b]pyrrole-5-carboxylic acid (106a)** (from **105a**): yield 98% (117 mg);
33 light brown solid. ^1H NMR ($\text{DMSO-}d_6$) δ (ppm): 12.48 (br s, 1 H), 7.62-7.47 (m, 1 H), 7.26-
34 7.19 (m, 1 H), 7.12 (s, 1 H), 3.99 (s, 3 H); MS (ESI): m/z : 180 [M-H].
35
36
37

38
39 **1-Methyl-4H-pyrrolo [2,3-d]imidazole-5-carboxylic acid (106f)** (from **104f**): yield 99%
40 (119 mg); MS (ESI): m/z : 166 [M+H] $^+$; MS (ESI): m/z : 164 [M-H].
41
42

43
44 **4-Ethylthieno[3,2-b]pyrrole-5-carboxylic acid (106m)** (from **105m**): yield 97% (230 mg);
45 brown solid. ^1H NMR ($\text{DMSO-}d_6$) δ (ppm): 12.46 (br s, 1 H), 7.62-7.46 (m, 1 H), 7.29-7.20
46 (m, 1 H), 7.16-7.07 (m, 1 H), 4.51 (q, $J= 7.3$ Hz, 2 H), 1.28 (t, $J= 6.8$ Hz, 3 H); MS (ESI):
47
48
49
50 m/z : 194 [M-H].
51

52
53 **4-Propylthieno[3,2-b]pyrrole-5-carboxylic acid (106n)** (from **105n**): yield 99% (200 mg);
54 colorless solid ^1H NMR ($\text{DMSO-}d_6$) δ (ppm): 12.43 (br s, 1 H), 7.60-7.44 (m, 1 H), 7.26-
55
56
57
58
59
60

1
2
3 7.20 (m, 1 H), 7.13 (s, 1 H), 4.50-4.33 (m, 2 H), 1.78-1.61 (m, 2 H), 0.85-0.72 (m, 3 H); MS
4
5 (ESI): m/z : 208 [M-H].
6

7 **4-Benzylthieno[3,2-b]pyrrole-5-carboxylic acid (106o)** (from **105o**): yield 100% (190 mg);
8
9 colorless solid, ^1H NMR (DMSO- d_6) δ (ppm): 12.54 (br s, 1 H), 7.62-6.95 (m, 8 H), 5.77 (s,
10
11 2 H); MS (ESI): m/z : 258 [M+H] $^+$.
12

13 **4-Phenylthieno[3,2-b]pyrrole-5-carboxylic acid (106p)** (from **105p**): yield 95% (110 mg);
14
15 beige solid; ^1H NMR (DMSO- d_6) δ (ppm): 12.44 (br s, 1 H), 7.62-6.69 (m, 8 H); MS (ESI):
16
17 m/z : 266 [M+Na].
18
19

20 **4H-Thieno[3,2-b]pyrrole-5-carboxylic acid (106r)** (from **105r**): yield quantitative, (180
21
22 mg); brown solid. ^1H NMR (DMSO- d_6) δ (ppm): 12.53 (br s, 1 H), 11.90 (br s, 1 H), 7.52-
23
24 7.35 (m, 1 H), 7.09-6.85 (m, 2 H); MS (ESI): m/z : 168 [M+H] $^+$.
25
26
27
28
29
30
31
32
33
34
35
36
37
38
39
40
41
42
43
44
45
46
47
48
49
50
51
52
53
54
55
56
57
58
59
60

ASSOCIATED CONTENT

Supporting Information. Synthetic procedures describing, **62-65, 83e-86e, 90e, 91e, 92-94**, additional figure illustrating the effects of KDM1A down regulation on mRNA expression of CD11b and CD14 in THP-1 cells, apoptotic induction assessment in THP-1 cells, data collection and refinement statistics for compound **19**, electron density map for compound **19**, interaction map for compound **19**, molecular formula strings (CSV). This material is available free of charge via the Internet at <http://pubs.acs.org> on the ACS Publications website at DOI:

Accession Codes

Atomic coordinates for the crystal structures of KDM1A with compound **19** can be accessed using PDB code 5LGN. Authors will release the atomic coordinates and experimental data upon article publication.

AUTHOR INFORMATION

Corresponding Author

* L.S. e-mail, luca.sartori@ifom.eu; phone, +39 02 9437 5121.

* P.V.: e-mail, paola.vianello@ifom.eu; phone, +39 02 9437 5030.

Notes

The authors declare no competing financial interest.

Present Addresses

§: IFOM – The FIRC Institute of Molecular Oncology, Experimental Therapeutics Unit, Via Adamello, 16. 20139 Milano. Italy.

#: Cogentech S.c.a.r.l. Via Adamello, 16. 20139 Milano. Italy.

¥: Nuevolution A/S, Rønnegade 8, DK-2100 Copenhagen. Denmark

ACKNOWLEDGMENT

1
2
3 This work was supported by Fondazione Cariplo (2010.0778), AIRC (**15208**), MIUR
4 (Progetto Epigen), FIRB RBFR10ZJQT and RF-2010-2318330 Projects by MIUR, Sapienza
5 Ateneo Project 2013, IIT-Sapienza Project, FP7 Projects BLUEPRINT/282510 and A-
6 PARADISE/602080, and Regione Lombardia, Fondo per la Promozione di Accordi
7 Istituzionale, Bando di Invito di cui al Decreto n. 4779 del 14/05/2009, Progetto DiVA,
8 BioStruct-X (FP7/2007-2013, grant agreement 283570) and Rasna Therapeutics Inc.
9

10 We thank scientists at the X06DA/PXIII beamline at the Swiss Light Source and the ID30A-
11 1/Massif-1 beamline at the European Synchrotron Radiation Facility for valuable help with
12 data collection.
13

14 ABBREVIATIONS

15
16 LSD, lysine-specific histone demethylase; MAO, monoamine oxidase; DIPEA, N,N-
17 diisopropylethylamine.; TLC, thin layer chromatography; AML, acute myeloid leukemia;
18 APL, acute promyelocytic leukemia; br s, broad signal; n-BuLi, n-butyllithium; CH₂Cl₂,
19 dichloromethane; DPPA, diphenylphosphoryl azide; DMEDA, 2-
20 (dimethylamino)ethylamine; MeOH, methanol; mp, melting point; PyBOP, (benzotriazol-1-
21 yloxy)tripyrrolidino- phosphonium hexa fluorophosphate; rt, room temperature; t-BuOH, tert-
22 butanol; TEA, triethylamine; THF, tetrahydrofuran
23
24
25
26
27
28
29
30
31
32
33
34
35
36
37
38
39
40
41
42
43
44
45
46
47
48
49
50
51
52
53
54
55
56
57
58
59
60

REFERENCES

- (1) Black, J. C.; Van Rechem, C.; Whetstone, J. R. Histone Lysine Methylation Dynamics: Establishment, Regulation, and Biological Impact. *Mol. Cell* **2012**, *48*, 491–507.
- (2) Greer, E. L.; Shi, Y. Histone Methylation: A Dynamic Mark in Health, Disease and Inheritance. *Nat. Rev. Genet.* **2012**, *13*, 343–357.
- (3) Huang, H.; Sabari, B. R.; Garcia, B. A.; David Allis, C.; Zhao, Y. SnapShot: Histone Modifications. *Cell* **2014**, *159*, 458–458e1.
- (4) Shi, Y.; Lan, F.; Matson, C.; Mulligan, P.; Whetstone, J. R.; Cole, P. A.; Casero, R. A.; Shi, Y. Histone Demethylation Mediated by the Nuclear Amine Oxidase Homolog LSD1. *Cell* **2004**, *119*, 941–953.
- (5) Lynch, J. T.; Harris, W. J.; Somerville, T. C. P. LSD1 Inhibition: A Therapeutic Strategy in Cancer? *Expert Opin. Ther. Targets* **2012**, *1*, 1–11.
- (6) Niebel, D.; Kirfel, J.; Janzen, V.; Holler, T.; Majores, M.; Gutgemann, I. Lysine-Specific Demethylase 1 (LSD1) in Hematopoietic and Lymphoid Neoplasms. *Blood* **2014**, *124*, 151–152.
- (7) Metzger, E.; Wissmann, M.; Yin, N.; Müller, J. M.; Schneider, R.; Peters, A. H. F. M.; Günther, T.; Buettner, R.; Schüle, R. LSD1 Demethylates Repressive Histone Marks to Promote Androgen-Receptor-Dependent Transcription. *Nature* **2005**, *437*, 436–439.
- (8) Lim, S.; Janzer, A.; Becker, A.; Zimmer, A.; Schüle, R.; Buettner, R.; Kirfel, J. Lysine-Specific Demethylase 1 (LSD1) Is Highly Expressed in ER-Negative Breast Cancers and a Biomarker Predicting Aggressive Biology. *Carcinogenesis* **2010**, *31*, 512–520.
- (9) Schulte, J. H.; Lim, S.; Schramm, A.; Friedrichs, N.; Koster, J.; Versteeg, R.; Ora, I.; Pajtler, K.; Klein-Hitpass, L.; Kuhfittig-Kulle, S.; Metzger, E.; Schule, R.; Eggert, A.; Buettner, R.; Kirfel, J. Lysine-Specific Demethylase 1 Is Strongly Expressed in Poorly

- 1
2
3 Differentiated Neuroblastoma: Implications for Therapy. *Cancer Res.* **2009**, *69*, 2065–
4
5 2071.
6
7
8 (10) Kahl, P.; Gullotti, L.; Heukamp, L. C.; Wolf, S.; Friedrichs, N.; Vorreuther, R.;
9
10 Solleder, G.; Bastian, P. J.; Ellinger, J.; Metzger, E.; Schüle, R.; Buettner, R.
11
12 Androgen Receptor Coactivators Lysine-Specific Histone Demethylase 1 and Four and
13
14 a Half LIM Domain Protein 2 Predict Risk of Prostate Cancer Recurrence. *Cancer Res.*
15
16 **2006**, *66*, 11341–11347.
17
18 (11) Lv, T.; Yuan, D.; Miao, X.; Lv, Y.; Zhan, P.; Shen, X.; Song, Y. Over-Expression of
19
20 LSD1 Promotes Proliferation, Migration and Invasion in Non-Small Cell Lung Cancer.
21
22 *PLoS One* **2012**, *7*, e35065.
23
24 (12) Zhao, Z. K.; Yu, H. F.; Wang, D. R.; Dong, P.; Chen, L.; Wu, W. G.; Ding, W. J.; Liu,
25
26 Y. Bin. Overexpression of Lysine Specific Demethylase 1 Predicts Worse Prognosis in
27
28 Primary Hepatocellular Carcinoma Patients. *World J. Gastroenterol.* **2012**, *18*, 6651–
29
30 6656.
31
32 (13) Wu, Y.; Wang, Y.; Yang, X. H.; Kang, T.; Zhao, Y.; Wang, C.; Evers, B. M.; Zhou, B.
33
34 P. The Deubiquitinase USP28 Stabilizes LSD1 and Confers Stem-Cell-like Traits to
35
36 Breast Cancer Cells. *Cell Rep.* **2013**, *5*, 224–236.
37
38 (14) Lee, M. G.; Wynder, C.; Schmidt, D. M.; McCafferty, D. G.; Shiekhattar, R. Histone
39
40 H3 Lysine 4 Demethylation Is a Target of Nonselective Antidepressive Medications.
41
42 *Chem. Biol.* **2006**, *13*, 563–567.
43
44 (15) Schmidt, D. M. Z.; McCafferty, D. G. Trans-2-Phenylcyclopropylamine Is a
45
46 Mechanism-Based Inactivator of the Histone Demethylase LSD1. *Biochemistry* **2007**,
47
48 *46*, 4408–4416.
49
50 (16) Thinnes, C. C.; England, K. S.; Kawamura, A.; Chowdhury, R.; Schofield, C. J.;
51
52
53
54
55
56
57
58
59
60
Hopkinson, R. J. Targeting Histone Lysine Demethylases - Progress, Challenges, and

- 1
2
3 the Future. *Biochim. Biophys. Acta - Gene Regul. Mech.* **2014**, *1839*, 1416–1432.
- 4
5 (17) Zheng, Y. C.; Ma, J.; Wang, Z.; Li, J.; Jiang, B.; Zhou, W.; Shi, X.; Wang, X.; Zhao,
6
7 W.; Liu, H. M. A Systematic Review of Histone Lysine-Specific Demethylase 1 and
8
9 Its Inhibitors. *Med. Res. Rev.* **2015**, *35*, 1032–1071.
- 10
11 (18) McGrath, J.; Trojer, P. Targeting Histone Lysine Methylation in Cancer. *Pharmacol.*
12
13 *Ther.* **2015**, *150*, 1–22.
- 14
15 (19) McAllister, T. E.; England, K. S.; Hopkinson, R. J.; Brennan, P. E.; Kawamura, A.;
16
17 Schofield, C. J. Recent Progress in Histone Demethylase Inhibitors. *J. Med. Chem.*
18
19 **2015**, *59*, 1308–1329
- 20
21 (20) Talele, T. T. The “Cyclopropyl Fragment” is a Versatile Player That Frequently
22
23 Appears in Preclinical/Clinical Drug Molecules. *J. Med. Chem.* **2016**, *59*, 8712–8756
- 24
25 (21) Ortega Munoz, A.; Fyfe, M. C. T.; Estiarte Martinez, M. d. L. A.; Valls Vidal, N.;
26
27 Kurz, G.; Castro Palomino, L. J. C. (Hetero)Aryl Cyclopropylamine Compounds as
28
29 LSD1 Inhibitors. WO2013/057320, **2013**.
- 30
31 (22) Mohammad, H. P.; Smitheman, K. N.; Kamat, C. D.; Soong, D.; Federowicz, K. E.;
32
33 Van Aller, G. S.; Schneck, J. L.; Carson, J. D.; Liu, Y.; Butticello, M.; Bonnette, W.
34
35 G.; Gorman, S. A.; Degenhardt, Y.; Bai, Y.; McCabe, M. T.; Pappalardi, M. B.;
36
37 Kaspavec, J.; Tian, X.; McNulty, K. C.; Rouse, M.; McDevitt, P.; Ho, T.; Crouthamel,
38
39 M.; Hart, T. K.; Concha, N. O.; McHugh, C. F.; Miller, W. H.; Dhanak, D.; Tummino,
40
41 P. J.; Carpenter, C. L.; Johnson, N. W.; Hann, C. L.; Kruger, R. G. A DNA
42
43 Hypomethylation Signature Predicts Antitumor Activity of LSD1 Inhibitors in SCLC
44
45 *Cancer Cell* **2015**, *28*, 57–69
- 46
47 (23) Investigation of GSK2879552 in Subjects With Relapsed/Refractory Small Cell Lung
48
49 Carcinoma
50
51
52 <https://clinicaltrials.gov/ct2/show/NCT02034123?term=GSK2879552&rank=1>.
- 53
54
55
56
57
58
59
60

[Accessed July 20, 2016]

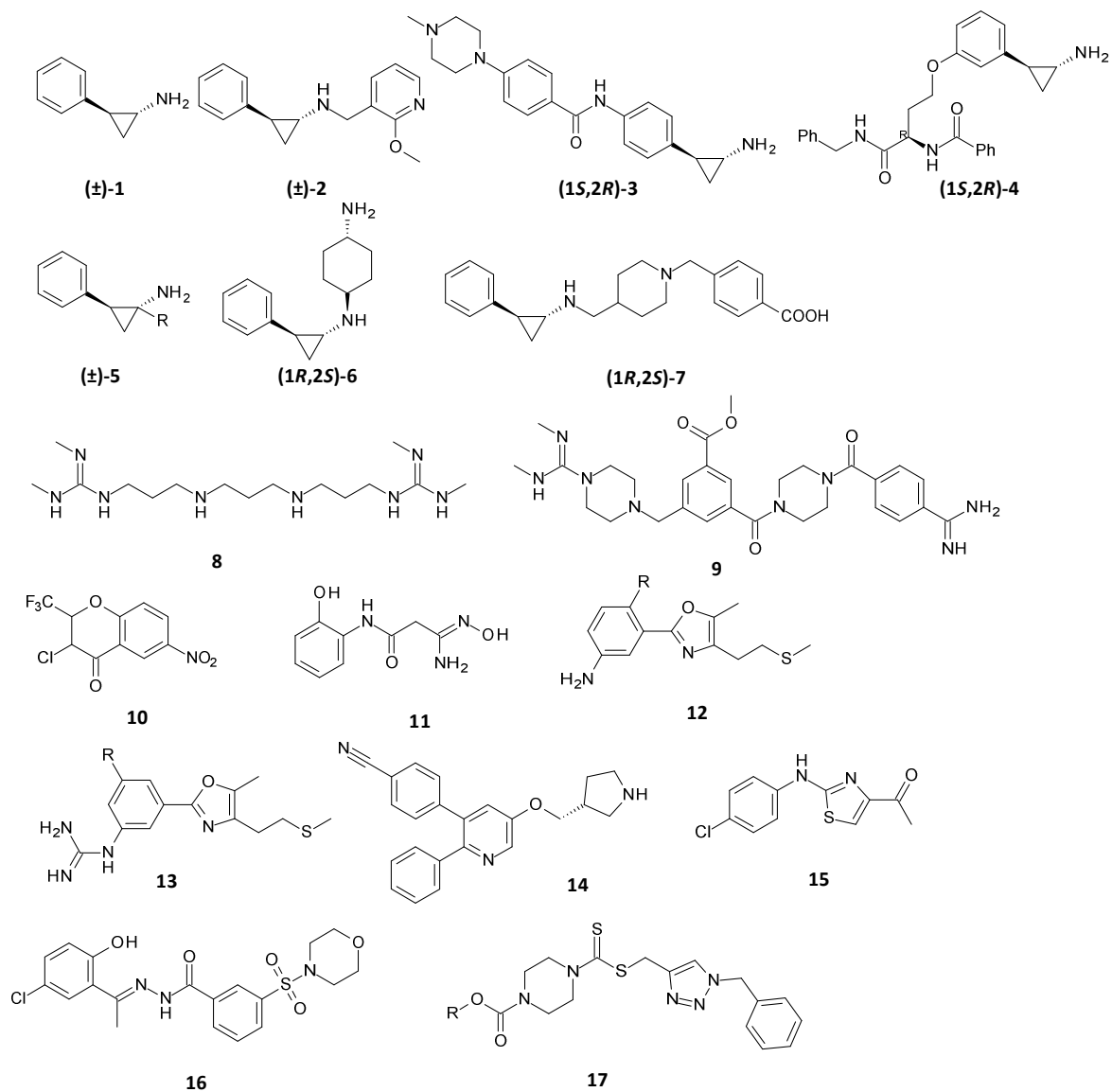
- (24) An Open-Label, Dose-Escalation/Dose-Expansion Safety Study of INCB059872 in Subjects With Advanced Malignancies
<https://clinicaltrials.gov/ct2/show/study/NCT02712905>. [Accessed October 7, 2016]
- (25) Vianello, P.; Botrugno, O. A.; Cappa, A.; Dal Zuffo, R.; Dessanti, P.; Mai, A.; Marrocco, B.; Mattevi, A.; Meroni, G.; Minucci, S.; Stazi, G.; Thaler, F.; Trifirò, P.; Valente, S.; Villa, M.; Varasi, M.; Mercurio, C. Discovery of a Novel Inhibitor of Histone Lysine-Specific Demethylase 1A (KDM1A/LSD1) as Orally Active Antitumor Agent. *J. Med. Chem.* **2016**, *59*, 1501–1517.
- (26) Mould, D. P.; McGonagle, A. E.; Wiseman, D. H.; Williams, E. L.; Jordan, A. M. Reversible Inhibitors of LSD1 as Therapeutic Agents in Acute Myeloid Leukemia: Clinical Significance and Progress to Date. *Med. Res. Rev* **2015**, *35*, 586–618.
- (27) Yu, V.; Fisch, T.; Long, A. M.; Tang, J.; Lee, J. H.; Hierl, M.; Chen, H.; Yakowec, P.; Schwandner, R.; Emkey, R. High-Throughput TR-FRET Assays for Identifying Inhibitors of LSD1 and JMJD2C Histone Lysine Demethylases. *J. Biomol. Screen.* **2012**, *17*, 27–38.
- (28) Vianello, P.; Sartori, L.; Amigoni, F.; Cappa, A.; Fagá, G.; Fattori, R.; Legnaghi, E.; Ciossani, G.; Mattevi, A.; Meroni, G.; Moretti, L.; Cecatiello, V.; Pasqualato, S.; Romussi, A.; Thaler, F.; Trifirò, P.; Vultaggio, S.; Varasi, M.; Mercurio, C. Thieno[3,2-B]pyrrole-5-Carboxamides as Novel Reversible Inhibitors of Histone Lysine Demethylase KDM1A/LSD1. Part 2: Structure Based Drug Design, SAR. *jm-2016-01019n in press*.
- (29) Baell, J.; Holloway, G. New Substructure Filters for Removal of Pan Assay Interference Compounds (PAINS) from Screening Libraries and for Their Exclusion in Bioassays. *J. Med. Chem.* **2010**, *53*, 2719–2740.

- 1
2
3 (30) Pouliot, M.; Jeanmart, S. Pan Assay Interference Compounds (PAINS) and Other
4 Promiscuous Compounds in Antifungal Research. *J. Med. Chem.* **2015**, *59*, 497–503.
5
6
7 (31) Malo, N.; Hanley, J. a; Cerquozzi, S.; Pelletier, J.; Nadon, R. Statistical Practice in
8 High-Throughput Screening Data Analysis. *Nat. Biotechnol.* **2006**, *24*, 167–175.
9
10
11 (32) BIOVIA Pipeline Pilot | Scientific Workflow Authoring Application for Data Analysis
12 <http://accelrys.com/products/collaborative-science/biovia-pipeline-pilot/>. [Accessed
13
14 July 20, 2016]
15
16
17
18 (33) Copeland, R. A. *Evaluation of Enzyme Inhibitors in Drug Discovery: A Guide for*
19 *Medicinal Chemists and Pharmacologists*; John Wiley & Sons, Inc., Hoboken, New
20
21
22
23
24
25
26 (34) Forneris, F.; Binda, C.; Adamo, A.; Battaglioli, E.; Mattevi, A. Structural Basis of
27
28
29
30
31
32 (35) Karasulu, B.; Patil, M.; Thiel, W. Amine Oxidation Mediated by Lysine-Specific
33
34
35
36
37
38
39 (36) Morris, G.; Huey, R. AutoDock4 and AutoDockTools4: Automated Docking with
40
41
42
43
44
45
46
47 (37) Korb, O.; Stütze, T.; Exner, T. E. Empirical Scoring Functions for Advanced Protein-
48
49
50
51
52
53
54
55
56
57
58
59
60
- (38) Friesner, R. A.; Banks, J. L.; Murphy, R. B.; Halgren, T. A.; Klicic, J. J.; Mainz, D. T.; Repasky, M. P.; Knoll, E. H.; Shelley, M.; Perry, J. K.; Shaw, D. E.; Francis, P.; Shenkin, P. S. Glide: A New Approach for Rapid, Accurate Docking and Scoring. 1. Method and Assessment of Docking Accuracy. *J. Med. Chem.* **2004**, *47*, 1739–1749.
- (39) Bottegoni, G.; Rocchia, W.; Recanatini, M.; Cavalli, A. ACIAP, Autonomous

- 1
2
3 Hierarchical Agglomerative Cluster Analysis Based Protocol to Partition
4 Conformational Datasets. *Bioinformatics* **2006**, *22*, e58–e65.
- 5
6
7 (40) Degliesposti, G.; Portioli, C.; Parenti, M. D.; Rastelli, G. BEAR, a Novel Virtual
8 Screening Methodology for Drug Discovery. *J. Biomol. Screen.* **2011**, *16*, 129–133.
- 9
10
11 (41) Heffernan, M. L. R.; Foglesong, R. J.; Hopkins, S. C.; Soukri, M.; Jones, S. W.; Spear,
12 K. L.; Varney, M. A. Fluoro-Substituted Inhibitors of D-Amino Acid Oxidase. U.S.
13 Patent 7,884,124 B2 **2008**.
- 14
15
16 (42) Ching, K. C.; Kam, Y. W.; Merits, A.; Ng, L. F. P.; Chai, C. L. L. Trisubstituted
17 thieno[3,2-B]pyrrole 5-Carboxamides as Potent Inhibitors of Alphaviruses. *J. Med.*
18 *Chem.* **2015**, *58*, 9196–9213.
- 19
20
21 (43) Harris, W. J.; Huang, X.; Lynch, J. T.; Spencer, G. J.; Hitchin, J. R.; Li, Y.; Ciceri, F.;
22 Blaser, J. G.; Greystoke, B. F.; Jordan, A. M.; Miller, C. J.; Ogilvie, D. J.; Somerville,
23 T. C. P. The Histone Demethylase KDM1A Sustains the Oncogenic Potential of MLL-
24 AF9 Leukemia Stem Cells. *Cancer Cell* **2012**, *21*, 473–487.
- 25
26
27 (44) Jin, L.; Hanigan, C. L.; Wu, Y.; Wang, W.; Park, B. H.; Woster, P. M.; Casero, R. A.
28 Loss of LSD1 (Lysine-Specific Demethylase 1) Suppresses Growth and Alters Gene
29 Expression of Human Colon Cancer Cells in a p53- and DNMT1(DNA
30 Methyltransferase 1)-Independent Manner. *Biochem. J.* **2013**, *449*, 459–468.
- 31
32
33 (45) Kerenyi, M. A.; Shao, Z.; Hsu, Y.-J.; Guo, G.; Luc, S.; O'Brien, K.; Fujiwara, Y.;
34 Peng, C.; Nguyen, M.; Orkin, S. H. Histone Demethylase Lsd1 Represses
35 Hematopoietic Stem and Progenitor Cell Signatures during Blood Cell Maturation.
36 *eLife* **2013**, *2*, e00633.
- 37
38
39 (46) Forneris, F.; Binda, C.; Battaglioli, E.; Mattevi, A. LSD1: Oxidative Chemistry for
40 Multifaceted Functions in Chromatin Regulation. *Trends Biochem. Sci.* **2008**, *33*, 181–
41 189.
- 42
43
44
45
46
47
48
49
50
51
52
53
54
55
56
57
58
59
60

- 1
2
3 (47) Binda, C.; Valente, S.; Romanenghi, M.; Pilotto, S.; Cirilli, R.; Karytinis, A.;
4
5 Ciossani, G.; Botrugno, O. A.; Forneris, F.; Tardugno, M.; Edmondson, D. E.;
6
7 Minucci, S.; Mattevi, A.; Mai, A. Biochemical, Structural, and Biological Evaluation
8
9 of Tranylcypramine Derivatives as Inhibitors of Histone Demethylases LSD1 and
10
11 LSD2. *J. Am. Chem. Soc.* **2010**, *132*, 6827–6833.
12
13
14 (48) Winn, M. D.; Ballard, C. C.; Cowtan, K. D.; Dodson, E. J.; Emsley, P.; Evans, P. R.;
15
16 Keegan, R. M.; Krissinel, E. B.; Leslie, A. G. W.; McCoy, A.; McNicholas, S. J.;
17
18 Murshudov, G. N.; Pannu, N. S.; Potterton, E. A.; Powell, H. R.; Read, R. J.; Vagin,
19
20 A.; Wilson, K. S. Overview of the CCP4 Suite and Current Developments. *Acta*
21
22 *Crystallogr., Sect. D Biol. Crystallogr.* **2011**, *67*, 235–242.
23
24
25 (49) SigmaPlot v11 <https://systatsoftware.com/products/sigmaplot/>. [Accessed July 20,
26
27 2016]
28
29
30 (50) Moretti, L; Sartori, L. Software Infrastructure for Computer-Aided Drug Discovery
31
32 and Development, a Practical Example with Guidelines. *Mol. Inf.* **2016**, *35*, 382–390.
33
34
35 (51) Seeliger, D.; De Groot, B. L. Ligand Docking and Binding Site Analysis with PyMOL
36
37 and Autodock/Vina. *J. Comput. Aided. Mol. Des.* **2010**, *24*, 417–422.
38
39
40 (52) A language and environment for statistical computing. R Foundation for Statistical
41
42 Computing <http://www.r-project.org/>. [Accessed July 20, 2016]
43
44
45 (53) D.A. Case, J.T. Berryman, R.M. Betz, D.S. Cerutti, T.E. Cheatham, III, T.A. Darden,
46
47 R.E. Duke, T.J. Giese, H. Gohlke, A.W. Goetz, N. Homeyer, S. Izadi, P. Janowski, J.
48
49 Kaus, A. Kovalenko, T.S. Lee, S. LeGrand, P. Li, T. Luchko, R. Luo, B. Madej, K.M.
50
51 Merz, G. Monard, P. Needham, H. Nguyen, H.T. Nguyen, I. Omelyan, A. Onufriev,
52
53 D.R. Roe, A. Roitberg, R. Salomon-Ferrer, C.L. Simmerling, W. Smith, J. Swails,
54
55 R.C. Walker, J. Wang, R.M. Wolf, X. Wu, D.M. York and P.A. Kollman (2015),
56
57 *AMBER 2015*, University of California, San Francisco.
58
59
60

- 1
2
3 (54) Pettersen, E. F.; Goddard, T. D.; Huang, C. C.; Couch, G. S.; Greenblatt, D. M.; Meng,
4
5 E. C.; Ferrin, T. E. UCSF Chimera--a Visualization System for Exploratory Research
6
7 and Analysis. *J. Comput. Chem.* **2004**, *25*, 1605–1612.
8
9
10 (55) Antonow, D.; Marrafa, T.; Dawood, I.; Ahmed, T.; Haque, M. R.; Thurston, D. E.;
11
12 Zinzalla, G. Facile Oxidation of Electron-Poor Benzo[b]thiophenes to the
13
14 Corresponding Sulfones with an Aqueous Solution of H₂O₂ and P₂O₅. *Chem. Commun.*
15
16 (*Camb*). **2010**, *46*, 2289–2291.
17
18
19
20
21
22
23
24
25
26
27
28
29
30
31
32
33
34
35
36
37
38
39
40
41
42
43
44
45
46
47
48
49
50
51
52
53
54
55
56
57
58
59
60

**Figure 1.** KDM1A Inhibitors

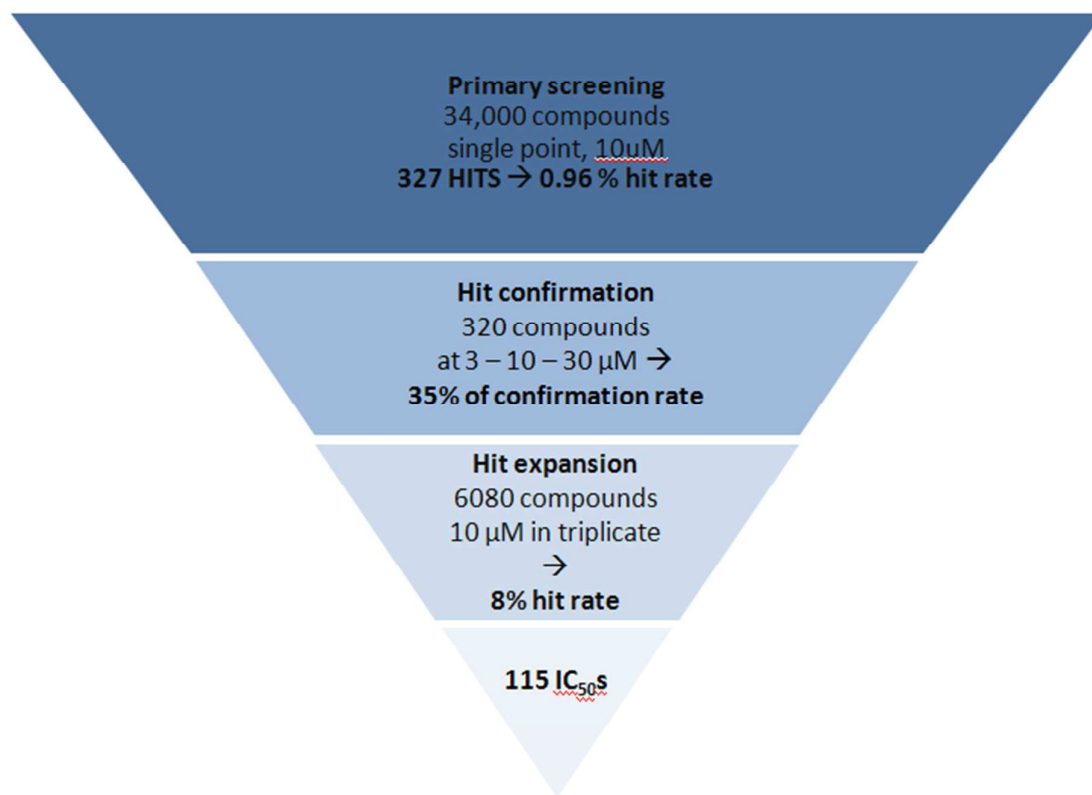
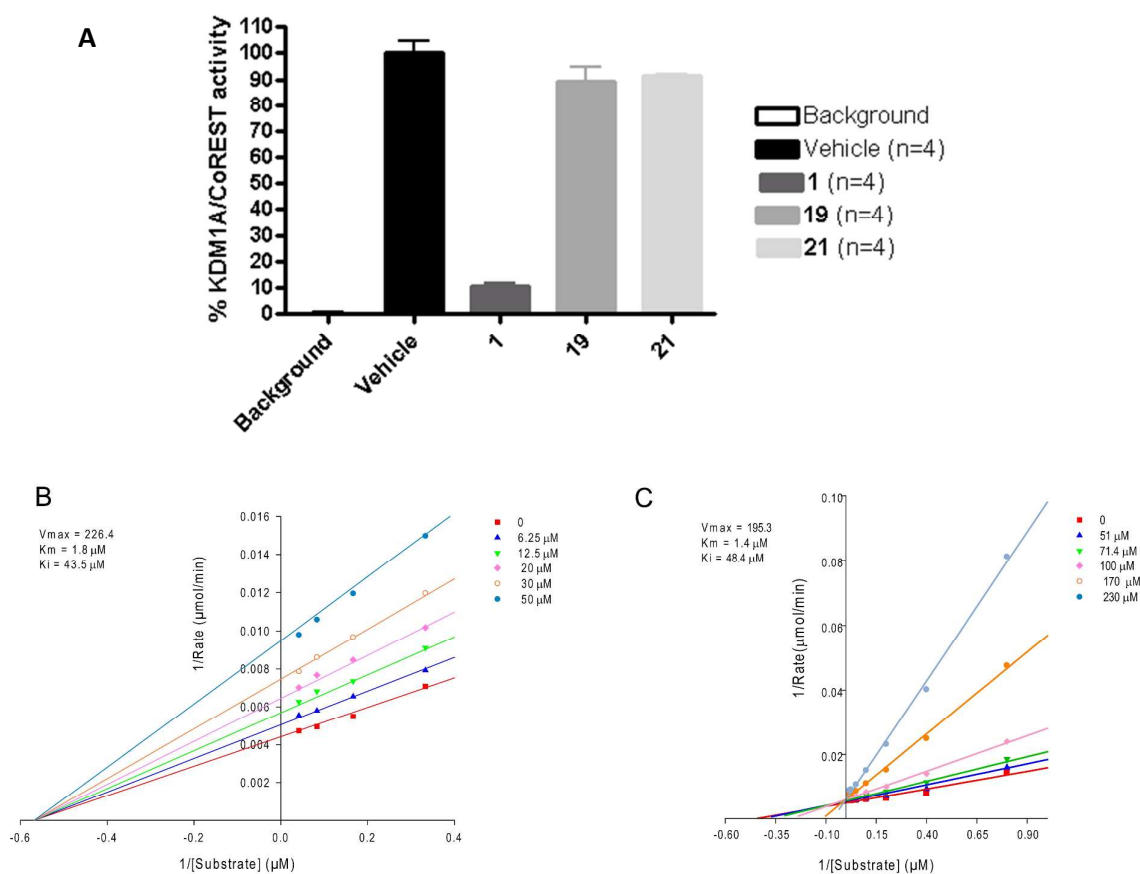


Figure 2. The HTS Workflow



37 **Figure 3.** (A) Compounds **19** and **21** reversibly inhibited KDM1A/CoREST enzymatic
38 activity. KDM1A/CoREST complex was incubated at a concentration 100 fold over
39 the concentration required for the enzymatic activity (2000 nM), with concentrations
40 of the inhibitors **19**, **21** and **1** equivalent to 10 fold of their IC_{50} s. After 15 minutes the
41 above solution is diluted 100 fold into reaction buffer containing the substrate to initiate
42 the reaction. **19** and **21**, contrarily to the irreversible inhibitor **1**, result in recovery of
43 enzymatic activity. (B): Plot of $1/(\text{Substrate})/1/\text{Rate}(\mu\text{mol}/\text{min})$ for a range of
44 concentration of **19**. (C): Plot of $1/(\text{Substrate})/1/\text{Rate}(\mu\text{mol}/\text{min})$ for a range of
45 concentration of **21**.

46
47
48
49
50
51
52
53
54
55
56
57
58
59
60

1
2
3
4
5
6
7
8
9
10
11
12
13
14
15
16
17
18
19
20
21
22
23
24
25
26
27
28
29
30
31
32
33
34
35
36
37
38
39
40
41
42
43
44
45
46
47
48
49
50
51
52
53
54
55
56
57
58
59
60

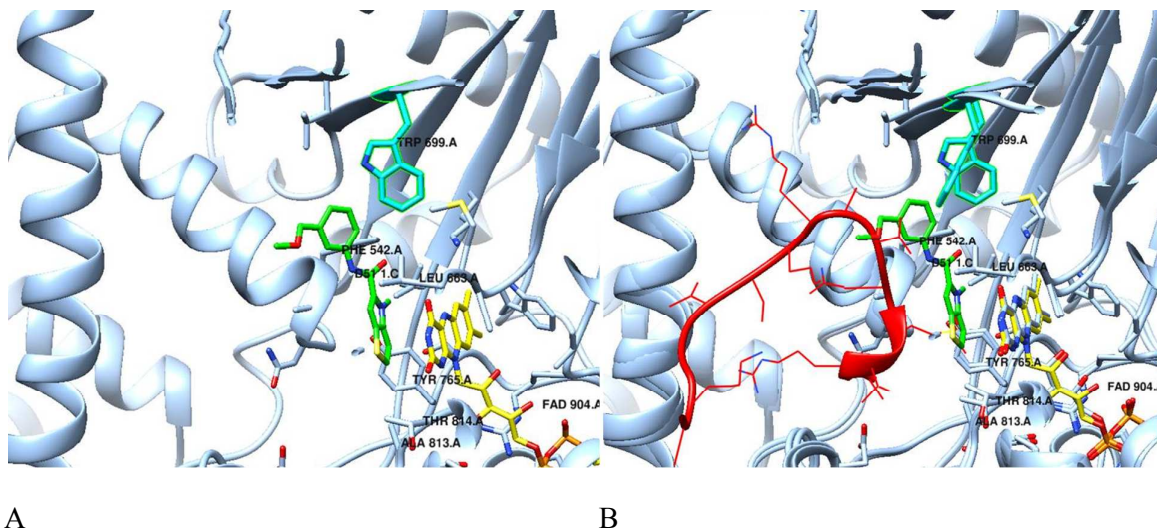


Figure 4. X-ray of 19: (A) Inhibitor interactions with target. **(B)** Comparison of crystallographic structure of 19 with KDM1A in complex with histone H3 peptide (2V1D): the superposition of the two structures shows the partial overlap of the thienopyrrole molecule with the atoms of the peptide. Trp699, in cyan, has shifted with respect to its reported position.

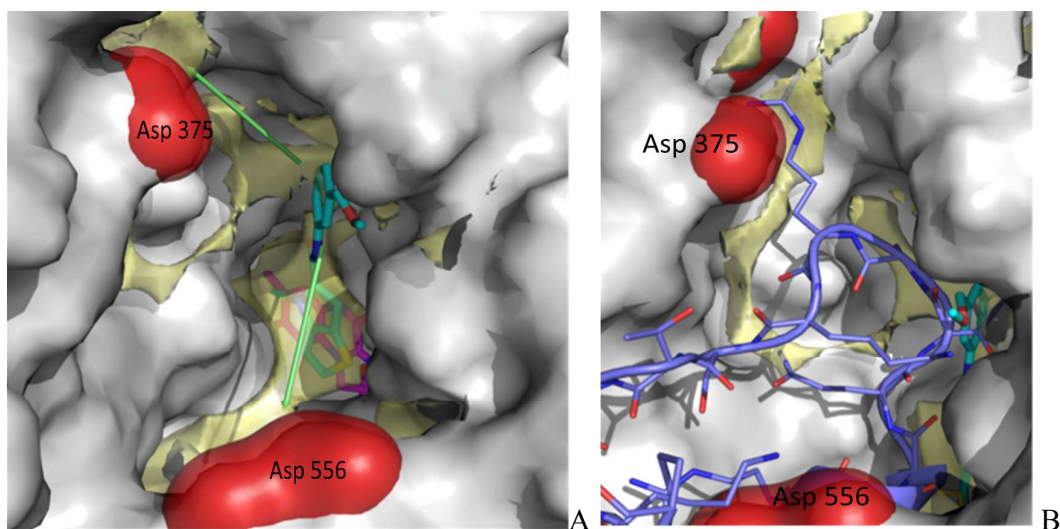


Figure 5. Favorable Interaction Regions.

The protein surface is displayed as well as the surfaces of the favorable interaction areas for hydrophobic character, in light-yellow, and for the electronegative ones, in red. **(A)** the inhibitor and cofactor molecules are in sticks representation and their carbon atoms are color-coded: cyan (inhibitor) and magenta (cofactor). In light-green 2 vectors are depicted from the position where the substituent emerges to the 2 electronegative regions. **(B)** the peptide substrate is depicted and some residues are visible in sticks with carbons in violet.

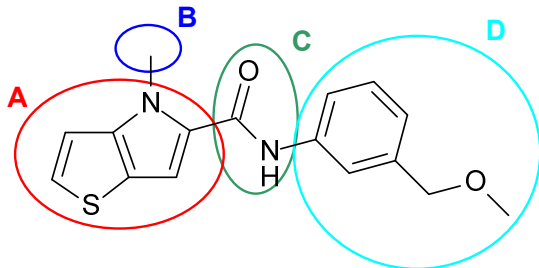


Figure 6. Four areas modified during Explorative SAR

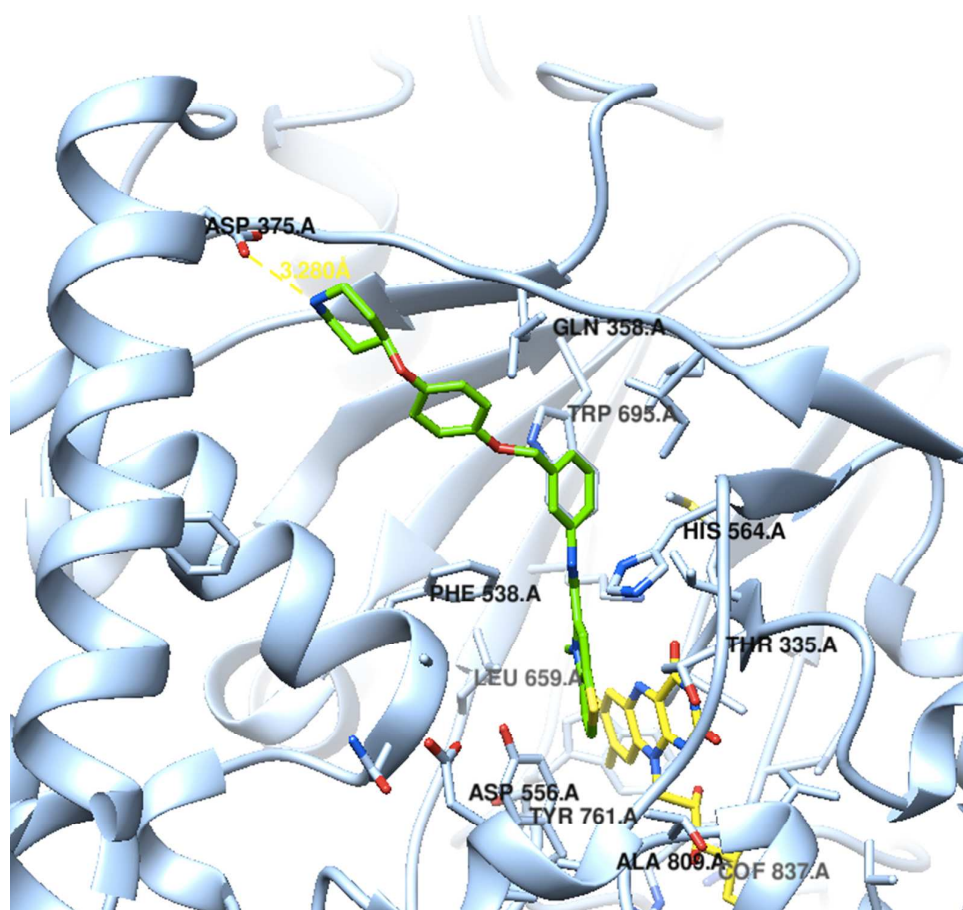


Figure 7. One of the accessible orientations for compound **90** in extended conformation with interactions with Asp375.

Table 1. HTS: Chemical Series With Inhibitory Activity

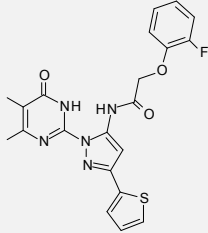
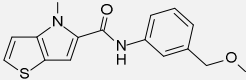
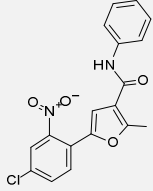
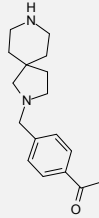
				
	18	19	20	21
IC₅₀ (μM)	0.76	2.9	3.5	5.0
Screened Analogues	141	56	4	43
Active Analogues	20	22	2	2
IC₅₀ < 50 μM	9	16	2	1

Table 2. Orthogonal Assay

Compound	TR-FRET HTS IC ₅₀ (μM)	TR-FRET IC ₅₀ (μM)	HRP IC ₅₀ (μM)
19	2.9	13.4±1.2	27.1±2.3
21	5.0	8.1±3.3	82.4±8.6
1		8.8±2.6	30.6 ±1.4

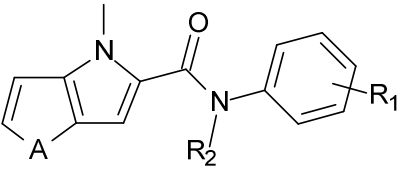
^a Data are expressed as the mean of at least two determinations ± standard deviation.

Table 3. Selectivity Profile of Compounds 19 and 21

Compound	KDM1A ^a IC ₅₀ (μM)	KDM1B ^a IC ₅₀ (μM)	MAOA ^a IC ₅₀ (μM)	MAOB ^a IC ₅₀ (μM)
19	13.4± 1.2	> 100	>100	56.8
21	8.1± 3.3	nd	>100	42.5
1	8.8±2.6	> 100	1.06±0.4	0.8±0.3

^a Data are expressed as the mean of at least two determinations ± standard deviation.

Table 4. Preliminary SAR

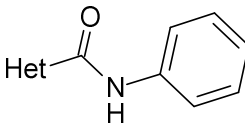
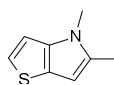
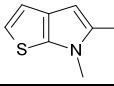
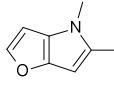
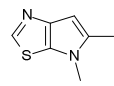
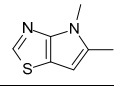
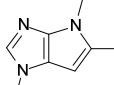
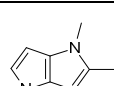
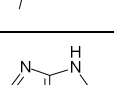
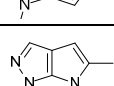
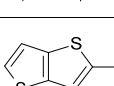
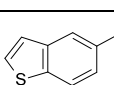
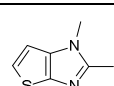


Compound	R ₁	position	Heteroatom (A)	R ₂	% Inhibition at 10 μM
19 ^b	CH ₂ OCH ₃	<i>m</i>	S	H	83
22	OCH ₃	<i>m</i>	S	H	58
23 ^b	H	//	S	H	49
24	F	<i>m</i>	S	H	48
25 ^b	CH ₂ OCH ₃	<i>m</i>	O	H	47
26	Cl	<i>m</i>	S	H	45
27	COOCH ₃	<i>m</i>	O	H	41
28 ^b	H	//	O	H	38
29	OCH ₃	<i>m</i>	O	H	36
30	CH ₂ SCH ₃	<i>m</i>	O	H	35
31	F	<i>o</i>	S	H	26
32	CH ₂ SCH ₃	<i>m</i>	S	H	22
33	OCH ₃	<i>o</i>	S	H	20
34	F	<i>o</i>	O	H	14
35	COCH ₃	<i>m</i>	O	H	13
36	OCH ₃	<i>o</i>	O	H	13
37	COCH ₃	<i>m</i>	S	H	11
38	H	//	S	CH ₃	6
39	Cl	<i>o</i>	O	H	4
40	H	//	O	CH ₃	3
41	Cl	<i>o</i>	S	H	inactive
42	COOCH ₃	<i>o</i>	O	H	inactive
43	COOCH ₃	<i>o</i>	S	H	inactive

^a All the compounds reported in table 4 have been purchased during chemical collection acquisition.

^b Compounds have also been synthesized according to Scheme 1.

Table 5. Heterocycle Variations

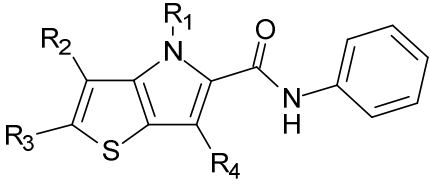
		
Compound ^b	Structure	IC ₅₀ (μM) ^a
23		25.7±3.4
45		38.8±2.0
28		89.5±6.2
46		>100
47		>100
48		>100
49		>100
50		>100
51		>100
52		>100
92		>100
93		>100

^a Data are expressed as the mean of at least two determinations ± standard deviation.

^b All the compounds have been prepared according to Scheme 1, except for **92**⁵⁵ and **93** (See Supporting Info for synthetic procedures).

1
2
3
4
5
6
7
8
9
10
11
12
13
14
15
16
17
18
19
20
21
22
23
24
25
26
27
28
29
30
31
32
33
34
35
36
37
38
39
40
41
42
43
44
45
46
47
48
49
50
51
52
53
54
55
56
57
58
59
60

Table 6. Ring Substitutions

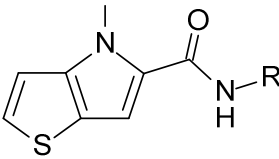


The chemical structure shows a thienopyridine core. The pyridine ring is fused to a thiophene ring. The nitrogen atom of the pyridine ring is substituted with R₁. The thiophene ring has substituents R₂ and R₃. The pyridine ring has a substituent R₄. A benzamide group (-C(=O)NH-Ph) is attached to the pyridine ring at the 2-position.

Compound	R ₁	R ₂	R ₃	R ₄	IC ₅₀ (μM) ^a
66	Et	H	H	H	9.3±2.6
23	Me	H	H	H	25.7±3.4
94	-CH ₂ CH ₂ NH ₂	H	H	H	48.1±5.6
67	Pr	H	H	H	53.2±17.3
44	Me	H	Br	H	>100
53	Me	H	Me	H	>100
54	Me	Me	H	H	>100
55	Me	Me	Me	H	>100
56	Me	H	H	Cl	>100
58	Me	H	H	I	>100
59	Me	H	I	H	>100
60	Me	H	I	I	>100
61	Me	H	F	H	>100
62	Me	H	H	-CH ₂ -OMe	>100
63	Me	H	H	Me	>100
64	Me	H	H	-CH ₂ -N(Me) ₂	>100
65	Me	H	-CH ₂ -N(Me) ₂	H	>100
68	Ph	H	H	H	>100
69	H	H	H	H	>100
70	PhSO ₂ -	H	H	H	>100

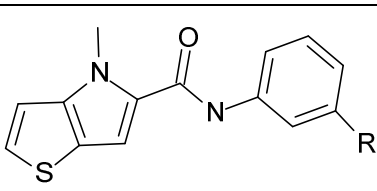
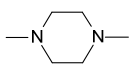
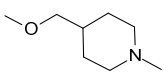
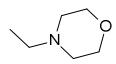
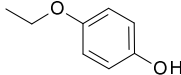
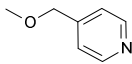
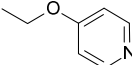
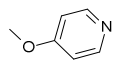
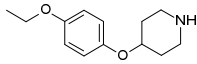
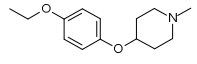
^a Data are expressed as the mean of at least two determinations ± standard deviation.

Table 7. Phenyl Replacement.

		
Compound	Structure	IC ₅₀ (μM) ^a
23		25.7±3.4
72		61.5±5.1
73		>100
74		>100
75		>100
76		>100

^a Data are expressed as the mean of at least two determinations ± standard deviation.

TABLE 8. *Meta* Substituents

			
Compound	R	IC ₅₀ (μM) ^a	
a	26	-Cl	18.7±3.78
	77		21.5±2.24
	24	-F	22.2±2.44
	23	-H	25.7±3.35
	22	-OCH ₃	26.5±4.22
	78	-N(Me) ₂	29.6±2.31
	79	-CONH ₂	97.3±13.8
	80	-Br	>100
b	81		2.2±0.9
	32	-CH ₂ SMe	7.4±0.2
	82		11.1±2.4
	19	-CH ₂ OMe	13.4±1.2
	83	-CH ₂ N(Me) ₂	16.7±0.2
	84		25.2±0.4
	85 86	-CH ₂ OH -CH ₂ OPh	52.3±8.0 >100
c	87		7.2±1.9
	88		9.4±1.3
	89		89.9±3.4
d	90		0.162±0.02
	91		0.442±0.03

^a Data are expressed as the mean of at least two determinations ± standard deviation.

Table 9: Biochemical and Cellular Characterization of Most Potent Derivatives.

Compound	KDM1A ^a IC ₅₀ (μM)	KDM1B ^a IC ₅₀ (μM)	MAOA ^a IC ₅₀ (μM)	MAOB ^a IC ₅₀ (μM)	CD14 ^b Fold increase	CD11b ^b Fold increase
90	0.16±0.02	>100	>100	7.16±3.5	4.79±0.2	4.61±0.2
91	0.44±0.03	>100	>100	7.60±6.1	2.76±0.2	4.76±0.3
ORY-1001^c	0.0006.0±0.0001	43.4±9.6	48.3±7.9	>100	5±0.3	11.1±1.45

^a Data are expressed as the mean of at least two determinations ± standard deviation.

^b Fold increase mRNA expression, reported as mean values of several replicates (≥ 2) at the fixed dose of 1 μM, measured after 24 h of compound treatment.

^c Fold increase mRNA expression, reported as mean values of several replicates (≥ 2) at the fixed dose of 0.5 μM, measured after 24 h of compound treatment

Table 10 Anticlonogenic potential of most potent derivatives

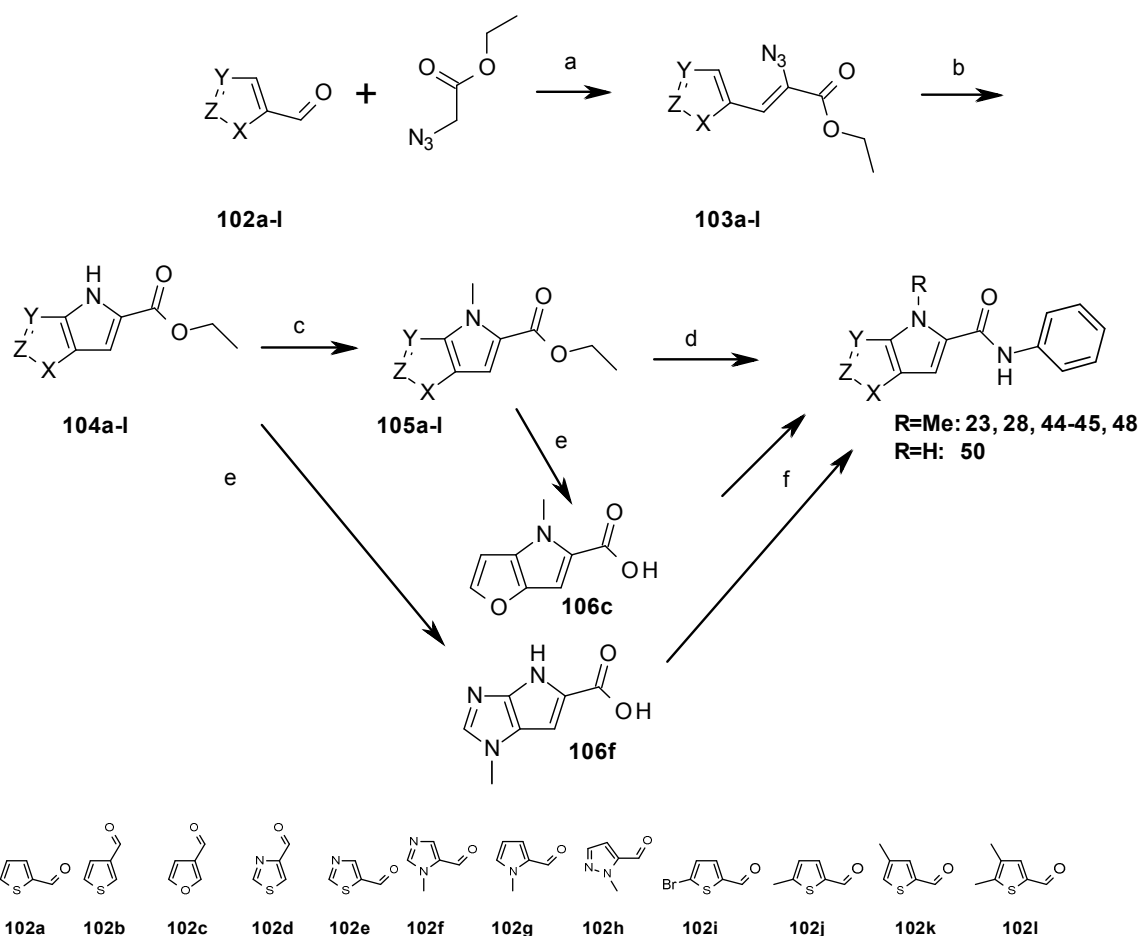
Compound	THP_1^a Colony formation inhibition	CD86 expression^b Fold increase
90^c	29.5±5	14.3±2.49
ORY-1001^d	70±2.8	55±8

^aColonies were counted after 13 days Percentage of inhibition is referenced to the vehicle (DMSO) treated cells, and the data reported are the mean of several replicates plus the standard deviation (≥ 2).

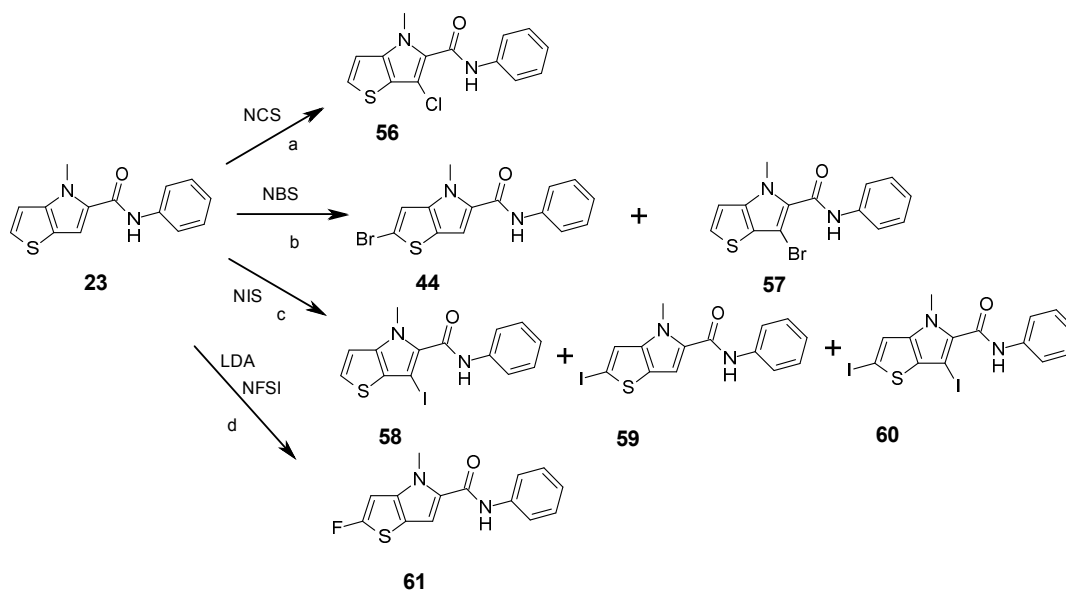
^b Fold increase mRNA expression, reported as mean values of several replicates (≥ 2) measured at the end of experiment

^cCompound was tested at the dose of 5 μ M

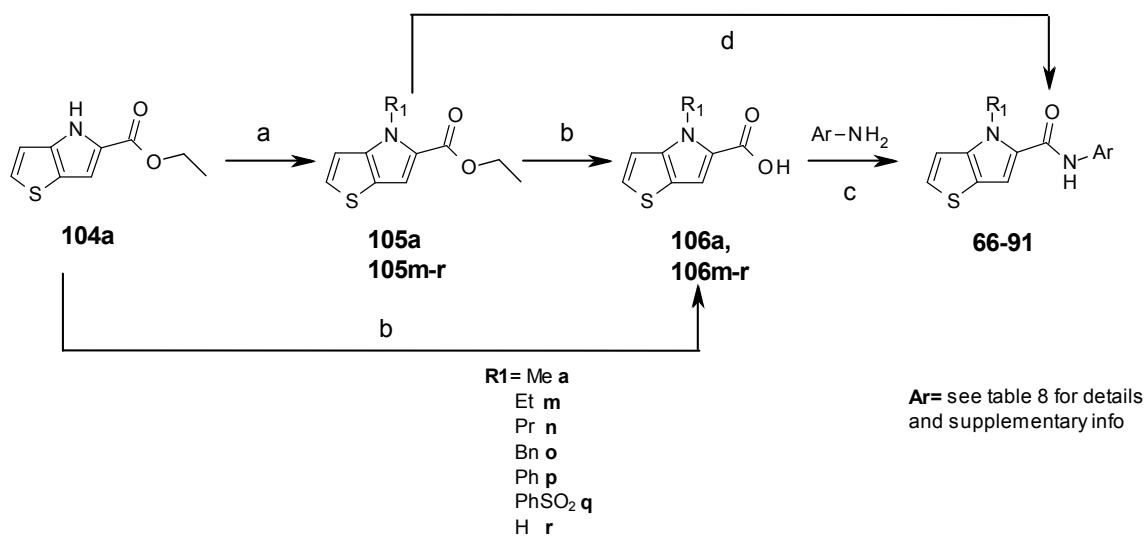
^dCompound was tested at the dose of 0.5 μ M

Scheme 1. General synthesis of 5-5 derivatives^a

^a Reagents and conditions: (a) EtOK, EtOH, 4h, 0°C to rt; (b) Xylene, reflux, 30 min; (c) (1) NaH, DMF, rt, 30min-1h, (2) MeI, rt; (d) PhNH₂ (up to 1.6 equiv.), LiHMDS (up to 2.6 equiv.), THF, 0°C to rt, 2h; (e) LiOH, H₂O/EtOH, rt 3 h; (f) (1) SOCl₂, DCM/THF, 2 h reflux, (2) PhNH₂, pyridine, rt, overnight.

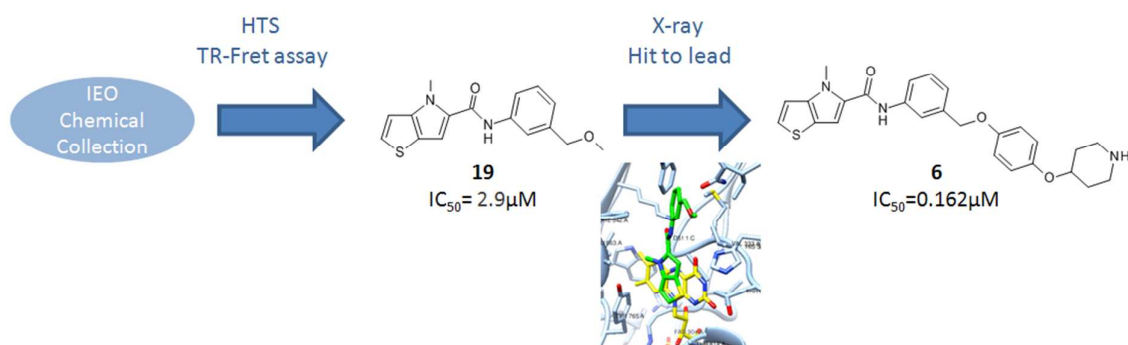
Scheme 2. Synthesis of halogenated thienopyrroles^a

^a Reagents and conditions: (a) NCS (1.05 equiv.), DCM, 0°C to rt overnight; (b) NBS (1.05 equiv), DCM, 0°C to rt overnight; (c) NIS (1.05 equiv), DCM 0°C to rt overnight, 18% **58**, 16% **59**, 2% **60**; (d) LDA (3 equiv), THF, -78°C, 1h; NFSI (3 equiv), -78°C to rt 1h.

Scheme 3.^a

^aReagents and Conditions. (a) i] NaH, DMF, rt, 30min-1h, then R1I, rt; or ii] phenylboronic acid Cu(OAc)₂, TEA, PYR; (b) LiOH, H₂O/EtOH, rt 3 hours; (c) (1) SOCl₂ (1.3 equiv), THF, 67°C 2h (2) Ar-NH₂ (**102a-z**, 0.6 equiv), pyridine, rt 90 min; (d) PhNH₂ (up to 1.6 equiv.), LiHMDS (up to 2.6 equiv.), THF, 0°C to rt, 2h;

Table of Contents Graphic



1
2
3
4
5
6
7
8
9
10
11
12
13
14
15
16
17
18
19
20
21
22
23
24
25
26
27
28
29
30
31
32
33
34
35
36
37
38
39
40
41
42
43
44
45
46
47
48
49
50
51
52
53
54
55
56
57
58
59
60